Russian Chemical Reviews **80** (9) 829 – 853 (2011) © 2011 Russian Academy of Sciences and Turpion Ltd

DOI 10.1070/RC2011v080n09ABEH004199

Isotrithionedithiolate transition metal complexes

V A Starodub, T N Starodub

Contents

I.	Introduction	829
II.	Methods for the synthesis of isotrithionedithiolate complexes	830
III.	Electronic and crystal structures of transition metal isotrithionedithiolates	832
IV.	Electrophysical properties of isotrithionedithiolate complexes	837
V.	Magnetic properties of isotrithionedithiolate complexes	845
VI.	Prospects of the practical use of isotrithionedithiolate complexes	849

Abstract. Methods for the synthesis and the electronic and crystal structures of neutral and anionic isotrithionedithiolate transition metal complexes are considered. The unusual electrophysical, magnetic and optical properties of these complexes, including superconducting structures, spin-ladder structures and nonlinear optical materials, are analyzed. The bibliography includes 129 references.

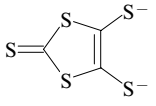
I. Introduction

Isotrithionedithiolate complexes (complexes with the 1,3-dithiol-2-thione-4,5-dithiolate ion, $C_3S_5^{2-}$, dmit) were described for the first time in fundamental studies by Steimecke and Wawzonek [1,2] (the abbreviation dmit originates from the obsolete name for the sulfur-containing heterocycle, dimercaptoisotrithione).

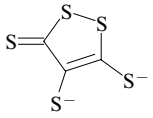
The reduction of carbon dioxide can give oxalates,[3] carbon monoxide, formic acid or methanol.[4] The authors of the studies [1,2] investigated the possibility of the synthesis of tetrathiooxalates by chemical (with alkali metals) [1] or electrochemical [2] reduction of carbon disulfide. In both cases, the reduction affords a cherry-red solution containing a mixture of trithiocarbonates and dmit:

$$4\,CS_2 + 4\,e^- \longrightarrow CS_3^{2-} + C_3S_5^{2-}. \qquad (1)$$

Depending on the reactions conditions, the isomeric product, the trithionedithiolate (dmt) ion, can be obtained.



dmit

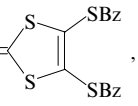


dmt

Since simple salts of the composition Ct_2dmit (Ct is a singly charged cation) are easily oxidized by atmospheric oxygen, zincate complexes $Ct_2[Zn(dmit)_2]$ have found use. The latter compounds are stable during storage in air and are readily involved in the exchange reactions with transition metal (M) salts or organic halogen derivatives to form both cyclic and linear addition products:

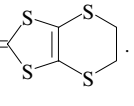
$$Ct_2[Zn(dmit)_2] + MHal_2 \longrightarrow Ct_2[M(dmit)_2] + ZnHal_2,$$

$$Ct_2[Zn(dmit)_2] + 4\,BzHal \longrightarrow Ct_2[ZnHal_4] + 2$$



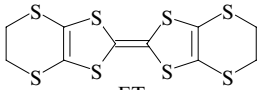
, (2)

$$Ct_2[Zn(dmit)_2] + 2\,HalCH_2CH_2Hal \longrightarrow Ct_2[ZnHal_4] + 2$$



.

The resulting thiones are convenient reagents for the synthesis of tetrathiafulvalene (TTF) derivatives, in particular, of bis(ethylenedithio)tetrathiafulvalene (ET).



ET

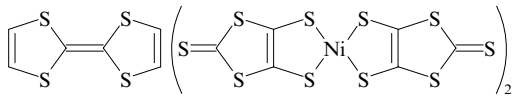
In the early 1980s, ET-based organic superconductors were synthesized.[5,6] Since that time, studies of ET radical cation salts (RCS) are going on.[7,8]

In 1986 the charge-transfer complex (CTC) of the composition $TTF[Ni(dmit)_2]_2$ was synthesized. This com-

V A Starodub, T N Starodub V N Karazin Kharkiv National University, pl. Svobody 4, 61077 Kharkiv, Ukraine, tel. (38-057) 340 30 91, e-mail: starodub@univer.kharkov.ua
Institute of Chemistry, Jan Kochanowski University of Humanities and Sciences, ul. Świętokrzyska 15 G , 25-406 Kielce, Poland (V A Starodub)

Received 1 December 2010
Uspekhi Khimii **80** (9) 865 – 889 (2011); translated by T N Safonova

plex exhibits metallic properties and undergoes a transition to the superconducting state at $T_C = 1.62$ K.[9]



$TTF[Ni(dmit)_2]_2$

Shortly after, superconductors based on mixed-valence dmit complexes, such as $(Me_4N)_{0.5}[Ni(dmit)_2]$[10] and b-$Me_4N[Pd(dmit)_2]_2$,[11] were synthesized. The properties of dmit complexes, including superconducting complexes, were described in 1999 in reviews.[12–14] In 2004 the monograph '*Dithiolene Chemistry. Synthesis, Properties, and Applications*' was published.[15] Unfortunately, certain issues were not included in these reviews. Besides, methods for the synthesis of dmit complexes were inadequately considered.

Considerable progress has been made in the chemistry of dmit complexes. In recent years, the nonlinear optical properties of dmit complexes have been discovered.[16–20] Besides, it was found that these complexes can form magnetically ordered structures, including spin ladders.[21, 22] In addition, dmit complexes can be used as near-infrared photodetectors. In 2000 superconducting Langmuir–Blodgett films based on the $(n\text{-}C_{14}H_{29})Me_3N[Au(dmit)_2]$ salt were discovered.[24] The fields of application of dmit complexes are considered in detail in the monograph.[15]

Hence, a new field of materials science has emerged ased on the chemistry of dmit and its analogues. This was the impetus for writing a review on the current state of the problem. The aim of the present study is to analyze the crystal structures of dmit complexes and the influence of the nature of transition metals and outer-sphere cations on their structures and the chemical, electrophysical, magnetic and optical properties. Emphasis is given to a comparative analysis of synthetic methods, because the industrial production of these complexes is an important problem.

II. Methods for the synthesis of isotrithionedithiolate complexes

There are currently two methods commonly used for the synthesis of dmit complexes.[12, 15] Both methods are based on the reduction of carbon disulfide with sodium in dimethylformamide according to the reaction (1). The salt Na_2dmit that formed is isolated from the reaction mixture and separated from sodium trithiocarbonate by the addition of the ammonium complex of zinc chloride (this is necessary because the reaction medium is highly alkaline).

$$2\,Na_2dmit + [Zn(NH_3)_4]Cl_2 \longrightarrow Na_2[Zn(dmit)_2] + 2\,NaCl + 4\,NH_3.$$

The zincate that formed is isolated from the reaction mixture by the addition of a solution of a salt with a large cation, because the solubility of dmit complexes decreases with increasing size of the outer-sphere cation. For this purpose, tetraethylammonium salts are most often used.

$$2\,Et_4NBr + Na_2[Zn(dmit)_2] \longrightarrow (Et_4N)_2[Zn(dmit)_2]\downarrow + 2\,NaBr.$$

After the separation of the precipitate of the complex salt, tetrabutylammonium salts are added to the mother solution. As a result, an additional amount of the complexes with a larger outer-sphere cation can be obtained, which leads to an increase in the total yield of the product.

$$2\,Bu^n_4NBr + Na_2[Zn(dmit)_2] \longrightarrow (Bu^n_4N)_2[Zn(dmit)_2]\downarrow + 2\,NaBr.$$

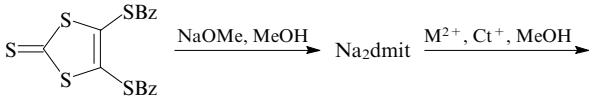
According to our estimates, the yield of ~60% can be obtained in this case. The complexes synthesized according to this procedure contain impurities of the isomeric complexes $Ct_2[Zn(dmit)(dmt)]$ and $Ct_2[Zn(dmt)_2]$. The product is purified by chromatographic methods.

The zinc complexes $Ct_2[Zn(dmit)_2]$ are then used for the synthesis of complexes with other transition metals.

$$Ct_2[Zn(dmit)v_2] + MX_2 \longrightarrow Ct_2[M(dmit)_2] + ZnX_2.$$

This reaction is efficient only if the metal (M) belongs to bases softer than zinc. For this reason, this method is unsuitable, for example, for the synthesis of manganates $Ct_2[Mn(dmit)_2]$. In addition, the method is inefficient in the synthesis of complexes with small outer-sphere cations. This is why this reaction is used primarily for the synthesis of complexes with such bulky outer-sphere cations, as tetraalkylammonium, tetraphenylphosphonium and tetraphenylarsonium.

An alternative method is based on the use of the dibenzoyl derivative of dmit, *viz*., 4,5-bis(benzoylthio)-1,3-dithiol-2-thione, which is generated in the reaction of $Ct_2[Zn(dmit)_2]$ complexes with benzoyl chloride [reaction (2)]. The dmit complexes are then synthesized according to the following scheme:



$$\longrightarrow Ct_2[M(dmit)_2].$$

The synthesis according to this procedures gives benzoic acid or its methyl ester as a by-product; the yield is determined by the yield of the zincate complex. The method includes three steps:[15] (1) the formation of the simple Na_2dmit salt by the reaction of the dibenzoyl thio derivative of dmit with a sodium methoxide solution; (2) the formation of a complex salt by the addition of an ethanolic or aqueous solution of a simple transition metal salt {for example, $NiCl_2 \cdot 6\,H_2O$; in this case, the complex salt $Na_2[Ni(dmit)_2]$ is obtained}; (3) the addition of an ethanolic or aqueous solution of a salt of the quaternary ammonium or phosphonium base. The $(Alk_4N)_2[M(dmit)_2]$ complex that precipitates is recrystallized from acetonitrile.

This method can be used also for the synthesis of the anhydrous complexes $Cs_2[M(dmit)_2]$ and $(Me_4N)_2$. $[M(dmit)_2]$ stable to atmospheric oxygen.[15]

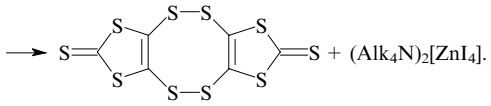
Based on these complexes, mixed-valence complexes can be synthesized. For this purpose, the oxidation with an iodine solution is used.

$$Ct_2[M(dmit)_2] + \frac{x}{2}\,I_2 \longrightarrow Ct_{2-x}[M(dmit)_2] + x\,CtI.$$

As was shown in 1989 by Neiland *et al.*,[25] the oxidation of $Ct_2[Zn(dmit)_2]$ complexes with an iodine solution affords isotrithionedithiol (C_6S_{10}, **1**), to which the polymeric structure $(C_3S_5)_x$ was assigned. According to our data,[26–28] this method gives isotrithionedithiol as a mixture of polymeric

and dimeric products, the content of the latter being increased as the temperature of the reaction mixture is lowered so that only the dimer is produced at temperatures below 0 °C.[27,28]

$$(Alk_4N)_2[Zn(dmit)_2] + 2\,I_2 \longrightarrow$$



$$+ (Alk_4N)_2[ZnI_4].$$

1

Dimer **1** adopts a chair conformation;[29] single crystals of **1** can be grown from a solution in benzene or carbon disulfide.

Five years after the publication of the study,[25] isotrithionedithiol was described by Rauchfuss and co-workers[29] (without referring to the studies of the predecessors); the authors synthesized this compound by the oxidation of the zincate complexes $Ct_2[Zn(dmit)_2]$ with sulfuryl chloride. In spite of the obvious drawbacks (the necessity of using thoroughly dried aprotic solvents, difficulties with the isolation), the method for the synthesis of isotrithionedithiolate with the use of sulfuryl chloride was described as the only method in the chapter 'Synthesis of Transition Metal Dithiolenes' written by Rauchfuss in the monograph.[15] The yield of the target product in this method was not higher than 74%,[29] whereas the use of iodide results in the nearly 100% yield.

The incorrect citation of the original publications in the monograph[15] led to subsequent incorrect references. For example, the authors of the study[30] synthesized isotrithionedithiol according to the method developed by Neiland *et al.*,[25] but they referred to Svenstrup and Becher.[31] In the same study, the authors used isotrithionedithiol for the preparation of alkyl derivatives of 4,5-ethylenedithio-1,3-dithiol-2-thione by the reaction of compound **1** with alkenes described in the study,[25] but referred to the study by Kini *et al.*[32] published in 1999.

The authors of the review published in 1994 discovered[26] the reaction of dimer **1** with hydrazine in an alkaline medium, which allows the preparation of dmit complexes with any outer-sphere cation and central atom in nearly 100% yields. Based on this reaction, a new efficient method for the synthesis of dmit complexes, which has virtually no limitations, was developed.[27,28] Since this method was not described in the reviews[12,13] and the monograph[15] [in the monograph,[15] it was only mentioned that the $(C_3S_5)_x$ polymer or the $(C_3S_5)_2^{2-}$ dianion can, in principle, be used for the synthesis of dmit complexes], let us briefly describe this procedure.

When performing the reduction of carbon disulfide with sodium, the temperature in the flask should be maintained below 0 °C (in this case, the isomeric product Na_2dmt does not form and there is no need in the chromatographic separation of isomers). After the completion of the reaction, a methanolic solution of iodine can be added, after quenching of an excess of sodium with methanol, directly to the reaction mixture until a yellow-brown precipitate of C_6S_{10}, which is almost insoluble in most of usual solvents, ceases to form. The dimer is poorly soluble only in carbon disulfide or benzene, from which it can be recrystallized to obtain crystals suitable for X-ray diffraction.

The dimer can be used for the synthesis of simple Ct_2dmit salts by the reaction

$$\underset{\mathbf{1}}{C_6S_{10}} + N_2H_4 + 4\,CtOH \longrightarrow 2\,Ct_2dmit + N_2\uparrow + 4\,H_2O.$$

As can be seen from the equation of the reaction, the solution contains the pure simple salt Ct_2dmit (this method can be used also for the preparation of Li_2dmit, which is most difficult to synthesize). These salts can be obtained in the pure form by distilling off a water–methanol mixture *in vacuo*.

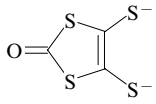
To synthesize dmit complexes, transition metal salts are added to the resulting solution:

$$2\,Ct_2dmit + MX_2 \longrightarrow Ct_2[M(dmit)_2] + 2\,CtX.$$

The yield of the $Ct_2[M(dmit)_2]$ complexes is close to 100% regardless of the nature of the outer-sphere cation (in other known methods, the smaller the outer-sphere cation, the lower the yield).

This method allowed us to synthesize for the first time the $Ct_2[M(dmit)_2]$ complexes, where M = Mn, Fe, Co, Cu, Hg; Ct = Li, Na, K, Rb, Cs,[28] which are difficult, if at all, to prepare by other methods.

It is interesting that the complexes of 1,3-dithiol-2-one-4,5-dithiolate (C_3OS_4, dmid) can also be obtained by this method.



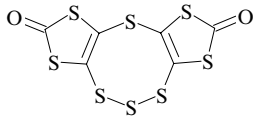
dmid

The dmid complexes are poorly known compared with the dmit complexes due mainly to the difficulties of their isolation from solution. For example, 425 dmit complexes and only 43 dmid complexes were described in the review.[13]

The oxidation of simple dmid salts with an iodine solution affords a pale-yellow precipitate of dione **2** ($C_6O_2S_8$):

$$2\,Na_2dmid + 2\,I_2 \longrightarrow 4\,NaI + \underset{\mathbf{2}}{C_6O_2S_8}.$$

Unlike C_6S_{10} (**1**), the latter dimer is unsymmetrical: two thiol rings are linked by sulfide bridges of different lengths.[29]



2

We showed[27] that this dimer is also easily reduced by hydrazine in an alkaline medium to form dmid salts:

$$\underset{\mathbf{2}}{C_6O_2S_8} + N_2H_4 + 4\,CtOH \longrightarrow 2\,Ct_2dmid + N_2\uparrow + 4\,H_2O.$$

The above-described method is suitable for the synthesis of both simple and complex salts $Ct_2[M(dmid)_2]$ in nearly 100% yield. Other methods can be used for the preparation of complexes only with bulky outer-sphere cations.

The oxidation of virtually all $Ct_2[M(dmit)_2]$ complexes (except for zincates) with a stoichiometric amount of iodine affords $Ct[M(dmit)_2]$ complexes. The reaction with an excess of iodine gives mixed-valence complexes, whose

composition depends on the nature of the outer-sphere cation. For example, the oxidation of the $Et_4N[Ni(dmit)_2]$ complex with an excess of iodine affords the complex of the composition $(Et_4N)_{0.5}[Ni(dmit)_2]$,[33] whereas the oxidation of the analogous complex containing the outer-sphere tetrabutylammonium cation gives the complex of the composition $(Bu^n_4N)_{0.29}[Ni(dmit)_2]$.[34–36] It should be noted that the $Ct_n[M(dmit)_2]$ complexes have primarily the 2 : 1 or 1 : 1 stoichiometry.[13] By contrast, it was shown[28] that complexes with small outer-sphere cations are characterized by a larger diversity of compositions (Table 1).

Table 1. Products of the reaction $Ct_2[M(dmit)_2] + I_2$.[28]

Ct	M	Complex	Ct	M	Complex
Li	Mn	$Li_{0.15}[Mn(dmit)_2]$	K	Co	$K[Co(dmit)_2]$
Na	Mn	$[Mn(dmit)_2]\cdot 1.5\,H_2O$	Rb	Co	$Rb[Co(dmit)_2]$
K	Mn	$K[Mn(dmit)_2]$	Cs	Co	$Cs[Co(dmit)_2]$
Rb	Mn	$Rb[Mn(dmit)_2]$	Li	Cu	$Li[Cu(dmit)_2]$
Cs	Mn	$Cs[Mn(dmit)_2]$	Na	Cu	$Na[Cu(dmit)_2]$
Li	Fe	$Li_{0.35}[Fe(dmit)_2]$	K	Cu	$K[Cu(dmit)_2]$
Na	Fe	$Na_{0.45}[Fe(dmit)_2]$	Rb	Cu	$Rb[Cu(dmit)_2]$
K	Fe	$K_{0.12}[Fe(dmit)_2]\cdot 2.5\,MeCN$,	Cs	Cu	$Cs[Cu(dmit)_2]$
		$K_{0.05}[Fe(dmit)_2]$	Li	Hg	$Li[Hg(dmit)_2]$
Rb	Fe	$[Fe(dmit)_2]\cdot 2\,MeCN$	Na	Hg	$Na[Hg(dmit)_2]$
Cs	Fe	$Cs_{0.5}[Fe(dmit)_2]$	K	Hg	$K[Hg(dmit)_2]$
Li	Co	$Li[Co(dmit)_2]$	Rb	Hg	$Rb[Hg(dmit)_2]$
Na	Co	$Na[Co(dmit)_2]$	Cs	Hg	$Cs[Hg(dmit)_2]$

The nickel complexes with small outer-sphere cations have some features different from those of the complexes containing large cations.[37] For example, the oxidation of a solution of the $Li_2[Ni(dmit)_2]$ complex in acetonitrile with a stoichiometric amount of an iodine solution affords the $Li[Ni(dmit)_2]$ complex. The oxidation of the latter complex in acetonitrile with an excess of iodine gives the complex of the composition $Li_{0.5}[Ni(dmit)_2]$, which is almost insoluble in acetonitrile, but is soluble in dimethylacetamide. The storage of this solution in air for two to three weeks results in the formation of long thin needles of the $Li_{0.27}[Ni(dmit)_2]$ complex. The latter is, in turn, almost insoluble in dimethylacetamide due to which the solution turns colorless.

In some cases, oxidized dmit complexes are formed immediately in the course of the synthesis. For example, in attempting to synthesize the $(Bu^n_4N)_2[Pt(dmit)_2]$ complex, the complex of formally trivalent platinum, $Bu^n_4N[Pt(dmit)_2]$, was isolated[38] due to the autooxidation (as the authors reported) of the initially formed $(Bu^n_4N)_2[Pt(dmit)_2]$ complex. We synthesized the same complex[39,40] by the autoreduction of the $[Pt(dmit)_2]$ complex, which was prepared by the reaction of $(Bu^n_4N)_2[Zn(dmit)_2]$ with $(Bu^n_4N)_2[PtCl_6]$. In this case, the term autoreduction is more correct because the complex of the formally tetravalent platinum is reduced with an excess of the $dmit^{2-}$ ion:

$$2\,[Pt(dmit)_2] + dmit^{2-} \longrightarrow 2\,[Pt(dmit)_2]^- + \frac{1}{2}\,(dmit)_2,$$

whereas in the study[38] this complex formed as a result of the oxidation with atmospheric oxygen.

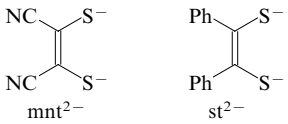
The synthesis of dmit complexes with the use of the Fe^{III} salts may lead to the formation of partially oxidized products in the case of small outer-sphere cations.[28] The compositions of the complexes prepared by the reaction of Ct_2dmit with iron(III) chloride are given below.

Ct	Complex
Li	$Li_{0.74}[Fe(dmit)_2]$
Na	$Na_{0.67}[Fe(dmit)_2]$
K	$K[Fe(dmit)_2]$
Rb	$Rb[Fe(dmit)_2]$
Cs	$Cs[Fe(dmit)_2]$

III. Electronic and crystal structures of transition metal isotrithionedithiolates

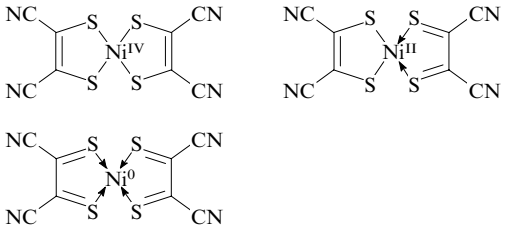
Most of dmit complexes belong to compounds, in which no particular oxidation state can be assigned to the central atom. This class of compounds includes the complexes of 2,2′-bipyridyl (bipy) with virtually any central atom.[41] For example, the neutral $[Li(bipy)_2]$, $[Be(bipy)_2]$, $[Al(bipy)_3]$ and $[Si(bipy)_3]$ complexes can be synthesized.

Transition metal alkenedithiolate complexes containing, for example, the 1,2-dicyanoethylenedithiolate ion (mnt^{2-}) or the stilbenedithiolate ion (st^{2-}) have similar properties.[42–44]



mnt^{2-} st^{2-}

These dithiolates react with transition metal salts to form $[ML_2]^{n-}$ complexes with n varying from 0 to 2. The problem of the electronic structure of these compounds may be illustrated by an example of the $[Ni(mnt)_2]$ complex. What oxidation state should be assigned to nickel in this complex? By considering different forms of the ligand, the nickel can have oxidation states from 0 to +4.



In 1960s, the electronic structures of alkenedithiolate complexes were extensively debated.[45,46] Finally, it was suggested that these complexes should be considered as metal-stabilized radical ionic systems.[44,47] In other words, the oxidation of $[ML_2]^{2-}$ complexes leads to a change in the electron density on all atoms of the complexes, while the electron density at the central atom may change only slightly. These complexes are still of interest to researchers (see, for example, the review[48]).

We face a similar problem when studying dmit complexes. Actually, it is hard to agree with the fact that, for example, cobalt, nickel or copper have the oxidation state +3 in complexes of the composition $Ct[M(dmit)_2]$. For the above-mentioned elements, this oxidation state is possible only in complexes with ligands containing highly electronegative elements. It is even less reasonable to assign the oxidation state +4 to nickel in the $[Ni(dmit)_2]$ complex described in the study.[34]

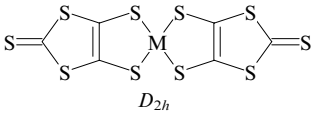
The electronic structure of $Ct_n[Ni(dmit)_2]$ complexes was investigated by X-ray photoelectron spectroscopy (XPS) and quantum chemical calculations using the X_α self-consistent field method in the relativistic approximation.[49] The bond energies of the ES2p and ENi2$p_{3/2}$ levels were measured depending on n and the nature of the outer-sphere cation. The calculations were performed for $[Ni(dmit)_2]^{n-}$ species. According to the results of calculations, the bond energies of 2p electrons of the nickel atom are virtually independent of the nature of the outer-sphere cation and the charge of the complex.

In addition, a change in the charge of the complex has almost no effect on the electron density at the nickel atoms. The oxidation of the complexes can even lead to an increase in the electron density at the nickel atoms. The latter fact can be easily explained by an increase in the conjugation in the ligand and an increase in the order of the donor-acceptor Ni—S bond.

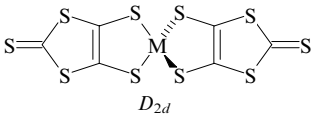
Hence, the $[M(dmit)_2]^{n-}$ complexes can be regarded in the same way as other dithiolate complexes. Thus, they can be considered as M^{II} complexes, and their oxidation may be related to the oxidation of the coordinated ligand. In this case, one would expect an increase in the conjugation of the coordinated dmit moieties through the orbitals of the central atom, which is favoured by the planar structure of the complexes.

An analysis of the data published in the literature shows[50,51] that $[Ni(dmit)_2]^{n-}$ complexes have a planar structure with the D_{2h} symmetry regardless of the n value. The data on the complexes with other central atoms are scarce, and there are only a few structurally characterized complexes. However, a knowledge of the structures of dmit complexes is important for the design of new materials for electronics based on these complexes. Thus, the mixed valence and the planar structure are necessary conditions for the formation of conducting complexes. If the structure is strongly nonplanar, the complexes have a loose packing. The dense packing provides a considerable overlap between orbitals of the complexes, and the mixed valence is responsible for the partial population of the band that formed, *i.e.*, of the conduction band.

We studied[28] the structures of the $Ct_n[M(dmit)_2]$ complexes (M = Mn, Fe, Co, Ni, Cu, Hg) by IR spectroscopy and quantum chemical calculation using the X_α (PB X_α) scattered wave method in the relativistic approximation for two conformations of the complexes, *viz.*, the planar (D_{2h}) and nonplanar (twisted, quasi-tetrahedral) (D_{2d}) with the metal in tetrahedral coordination. The well-known nickel complexes were taken to validate the predictions of quantum chemical calculations.



D_{2h}



D_{2d}

The symmetry of $Ct_n[M(dmit)_2]$ complexes can be determined from the analysis of their IR spectra.[28] In the case of the planar structure of the $[M(dmit)_2]$ complex, 45 vibrational degrees of freedom are distributed over the symmetry types as follows (the spectra, in which the corresponding vibrations are active, are given under the symbols of the symmetry types):

$$G = 8A_g \oplus 3A_u \oplus 7B_{1g} \oplus 5B_{1u} \oplus 2B_{2g} \oplus 8B_{2u} \oplus 4B_{3g} \oplus 8B_{3u}.$$
$$\text{Raman} \quad \text{Raman IR} \quad \text{Raman IR} \quad \text{Raman IR}$$

Hence, the IR spectrum of the planar $[M(dmit)_2]$ complex shows 21 lines, the same number of lines is observed in the Raman spectrum; however, none of these lines is observed in both spectra simultaneously (the rule of mutual exclusion).

For the twisted conformation, there is the following distribution of the symmetry vibrational modes:

$$G = 7A_1 \oplus A_2 \oplus 4B_1 \oplus 9B_2 \oplus 12E,$$
$$\text{Raman} \quad \text{Raman} \quad \text{IR, Raman} \quad \text{IR, Raman}$$

whereas the IR spectrum of the quasi-tetrahedral structure shows 21 lines, and all of them are Raman active as well; the Raman spectrum shows additional 11 lines. Hence, a comparison of the IR and Raman spectra of $[M(dmit)_2]^{n-}$ complexes is sufficient for the determination of their symmetry.

The vibrational frequencies depend in a certain way on the charge n of the complex. The dependence of the frequency of totally symmetric vibrations A_g for the planar structures (D_{2h}) of the $[Ni(dmit)_2]^{n-}$ and $[Pd(dmit)_2]^{n-}$ complexes on the charge n was analyzed.[52] Table 2 gives the A_g-type vibrational frequencies of the above-mentioned complexes with different n.

Table 2. Vibrational frequencies A_g (in cm^{-1}) for $[Ni(dmit)_2]^{n-}$ complexes.[52]

n	A_g1	A_g2	A_g3	A_g4	A_g5	A_g6	A_g7	A_g8
$[Ni(dmit)_2]^{n-}$								
0	1329	1051	950	496	488	364	343	140
0.3	1346	1055	—	504	486	363	344	138
0.5	1357	1071	946	513	481	360	340	134
1	1403	1052	933	507	478	358	338	137
2	1435	1046	907	521	466	351	323	128
$[Pd(dmit)_2]^{n-}$								
0.5	1354	1078	—	515	485	364	345	140
1	1400	1053	924	515	476	363	342	129
2	1445	1054	900	525	466	355	338	123

As can be seen from Table 2, only the frequency of the A_g1 vibration in both complexes depends in a particular way on the charge of the complexes. Based on the analysis of the Raman spectra of the planar $[M(dmit)_2]^{n-}$ complexes, this vibration is assigned to vibrations of the C=C bond.[52] The linear dependence is observed for the A_g1 vibrational frequency (in cm^{-1}) for the $[Ni(dmit)_2]^{n-}$ complexes

$$\tilde{\nu} = 1332 + 54.7n \ (R = 97.8\%),$$

and for the $[Pd(dmit)_2]^{n-}$ complexes

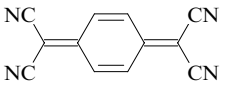
$$\tilde{\nu} = 1336.5 + 51.3n \ (R = 96.4\%).$$

Therefore, the charge of the complex can be determined from the measured A_g1 vibrational frequency . The vibrations of A_g symmetry are forbidden in the IR spectra because they have zero electric dipole transition moments. However, the situation changes if crystals of the complexes

have substantial electrical conductivity. In this case, the totally symmetric vibrations are not only observed but are also the most intense in the IR spectra.

The main ideas of the theoretical interpretation of this phenomenon were formulated in 1961 in the study by Fano,[53] who considered an abstract problem on the interaction of a discrete spectrum with a continuum and showed that this interaction gives sharp characteristic asymmetric peaks in the excitation spectrum manifested as resonances or antiresonances.

This phenomenon was observed for the first time in the IR spectra of the conducting 7,7,8,8-tetracyanoquinodimethane (TCNQ) radical anion salts (RAS).

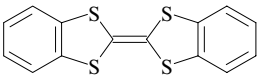


TCNQ

The vibrational structure lines for these RAS are observed against the background of an electronic continuum (corresponding to intra- and interband transitions). In addition, there are broad, abnormally intense (10–100 times more intense than normal absorption bands) lines, which are absent in the IR spectra of TCNQ and its poorly conducting RAS. Figure 1 shows the IR spectra of TCNQ radical anion salts of different types.

The theory of IR spectra of highly conducting TCNQ radical anion salts was developed in the studies.[55–58] Based on the study by Fano,[53] the authors of these investigations showed that in TCNQ-based narrow-band semiconductors or metals, the conduction electrons, whose wave vectors are polarized along the stack of radical anions, interact with totally symmetric vibrations A_g of TCNQ. In this case, the IR-inactive vibrations A_g become active. The excitation of intramolecular vibrations of A_g symmetry is accompanied by emission or absorption of acoustic phonons involved in the energy transfer from electronic excitations to intramolecular vibrations of A_g symmetry.

More recently, we observed [59] a similar effect in the IR spectra of dibenzotetrathiafulvalene (DBTTF)-based radical anion salts (narrow-band semiconductors or metals).



DBTTF

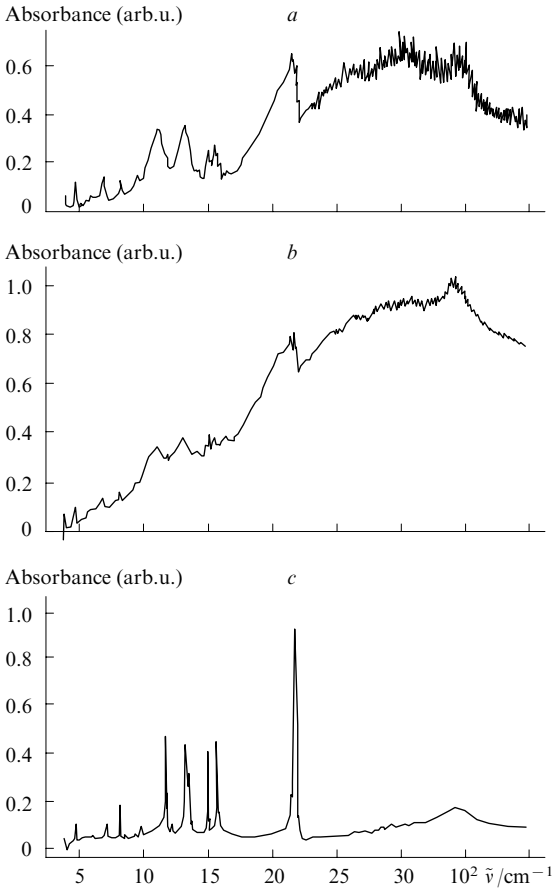


Figure 1. IR absorption spectra of radical anions salts.[54] (*a*) (*N*-Mepyz)(TCNQ)$_2$, metal; (*b*) (*N*-Mepyz)(TCNQ), a narrow-band semiconductor; (*c*) (*N*-Bu^{i}pyz)(TCNQ)$_2$, dielectric (pyz is pyrazine).

Based on quantum chemical calculations of the electron–phonon coupling (EPC) constants, the characteristic features of the IR spectra of highly conducting DBTTF radical cation salts were interpreted as interactions between intramolecular vibrations of the $DBTTF^{+\bullet}$ radical cation and excitations of conduction holes.[59]

Similar features are observed in the IR spectra of highly conducting dmit-based complexes. The EPC constants for crystals of the complexes containing the $[Ni(dmit)_2]^{n-}$ anions were calculated.[60] Figure 2 shows the modes of

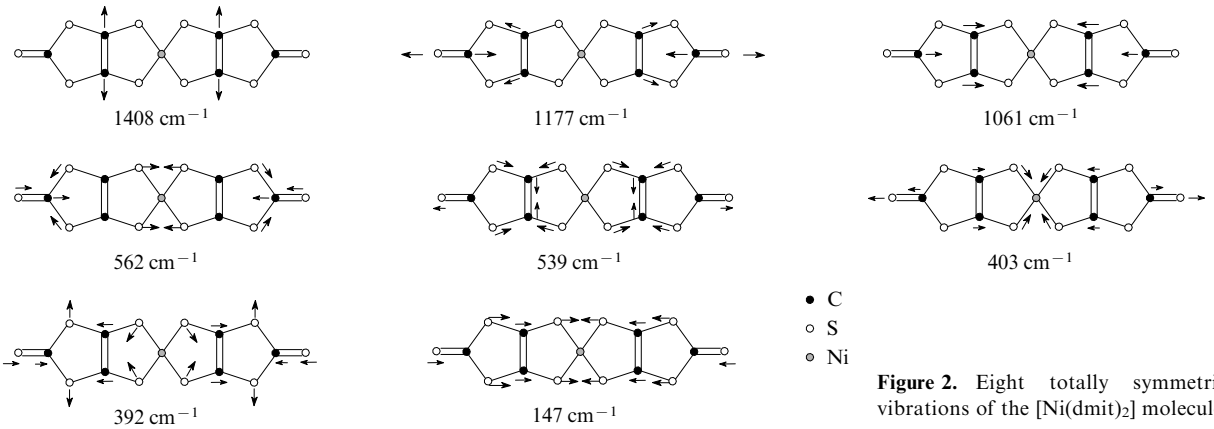


Figure 2. Eight totally symmetric (A_g) vibrations of the $[Ni(dmit)_2]$ molecule.[60]

eight totally symmetric vibrations (A_g symmetry) of the [Ni(dmit)$_2$] molecule.

As can be seen from Fig. 2, the A_g1 vibration (1408 cm^{-1}) corresponds to displacements of the carbon atoms of the C=C bond. As mentioned above, it is this vibration that is sensitive to the charge of the [Ni(dmit)$_2$]$^{n-}$ anion. Hence, it is not surprising that this vibration is characterized by the largest EPC constant.

The EPC constants for the highest occupied molecular orbital (HOMO) and the lowest unoccupied molecular orbital (LUMO) of the [Ni(dmit)$_2$] molecule were calculated.[60] The results are given in Table 3. As can be seen from Table 3, both theoretical and experimental values of the EPC constants are clearly indicative of the domination of the A_g1 vibration, for which this constant is an order of magnitude larger than those for the other vibrations. From these data, the maximum possible temperature of the transition to the superconducting state of [Ni(dmit)$_2$]-based complexes can be estimated. This estimation was made in the study:[60] $T_C \leqslant 11$ K.

Table 3. Electron–phonon coupling constants for HOMO and LUMO of the [Ni(dmit)$_2$] complex.

Calculations[60]			Experiment[61]	
$\tilde{\nu}$ /cm^{-1}	λ_{HOMO}	λ_{LUMO}	$\tilde{\nu}$ /cm^{-1}	λ_{LUMO}
1408	0.1260	0.1007	1296	0.0321
1177	0.0067	0.0044	1053	0.0036
1061	0.0007	0.0086	930	0.0049
562	0.0235	0.0072	–	–
539	0.0211	0.0122	512	0.0036
403	0.0235	0.0010	359	0.0076
392	0.0200	0.0253	335	0.0193
147	0.0024	0.0128	137	0.0226

The total electronic energy of the complexes can be used for the theoretical determination of the symmetry of these complexes. The total energy differences [$\Delta E = E(D_{2h}) - E(D_{2d})$] for two structures of the complexes are given below.[28]

Complex	ΔE /eV	Complex	ΔE /eV
[Mn(dmit)$_2$]$^{2-}$	−0.486	[Ni(dmit)$_2$]$^{2-}$	0.010
[Mn(dmit)$_2$]$^{-}$	−0.008	[Ni(dmit)$_2$]$^{-}$	−0.043
[Fe(dmit)$_2$]$^{2-}$	0.839	[Cu(dmit)$_2$]$^{2-}$	0.082
[Fe(dmit)$_2$]$^{-}$	0.025	[Cu(dmit)$_2$]$^{-}$	0.110
[Co(dmit)$_2$]$^{2-}$	−0.027	[Hg(dmit)$_2$]$^{2-}$	0.217
[Co(dmit)$_2$]$^{-}$	0.016	[Hg(dmit)$_2$]$^{-}$	0.213

As can be seen from the above data, the calculations correctly predict the higher stability of the planar structure of the [Ni(dmit)$_2$]$^{n-}$ complexes: a somewhat lower stability of the planar structure of the [Ni(dmit)$_2$]$^{2-}$ complex may be compensated by the Madelung energy gain due to the closer packing of the planar complexes.

The planar structures of manganate complexes are more stable in both charge states. According to scarce structural data for [Mn(dmit)$_2$]$^{n-}$ complexes,[62] they have a more intricate (dimeric) structure. For example, the $(Me_4N)_4[Mn_2(dmit)_4]$ complex consists of two fragments linked by donor–acceptor Mn–S bonds (Fig. 3), resulting in the distorted trigonal-bipyramidal coordination of the

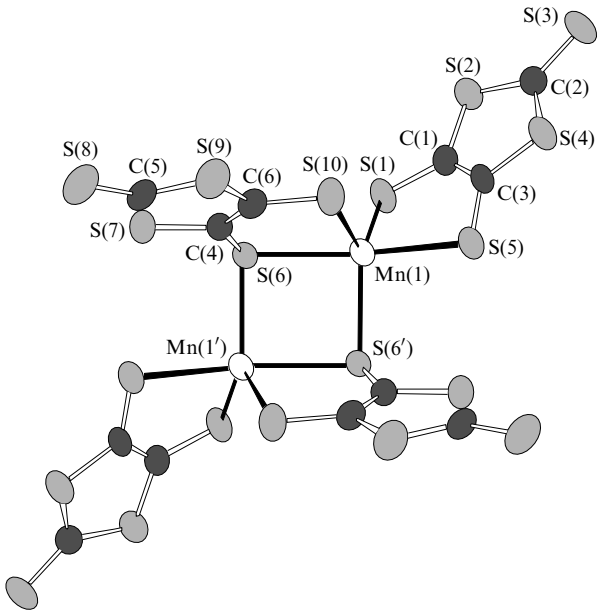


Figure 3. Structure of the anion in the $(Me_4N)_4[Mn_2(dmit)_4]$ complex.[62]

Mn^{II} ion. However, the contradiction with the results of our calculations can be easily explained. Thus, the energy difference between LUMO and HOMO is so small that the [Mn(dmit)$_2$]$^{n-}$ complexes can be readily transformed into the excited biradical state (due to thermal excitation), which accounts for their dimerization. Similar ideas were invoked to explain the dimerization of the [Pd(dmit)$_2$]$^{n-}$ complexes.[63,64]

It is hardly possible to synthesize planar complexes containing the [Fe(dmit)$_2$]$^{2-}$ anion. As can be seen from the values of ΔE, the twisted conformation is much more stable than the planar structure. However, the energy difference between the two structures of the [Fe(dmit)$_2$]$^{-}$ complexes is much smaller (0.025 eV), due to which the less stable planar structure can be stabilized in the crystalline state. This is consistent with experimental data.[15,51]

As for the [Co(dmit)$_2$]$^{n-}$ complexes, they can have a planar structure in both charge states, as is evident from the

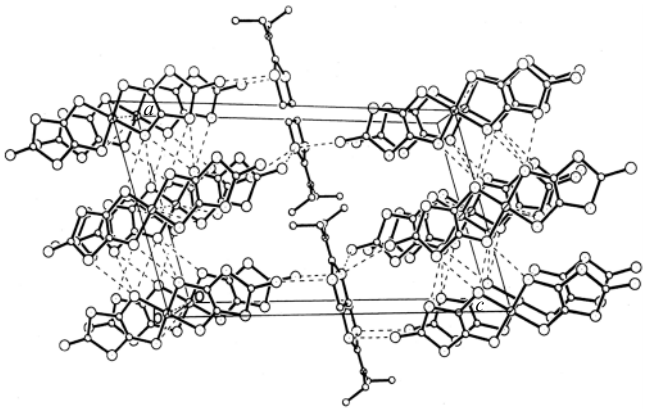


Figure 4. Crystal structure of the EDA[Ni(dmit)$_2$]$_3$ complex. The S···S contacts shorter than the sum of the van der Waals radii[69] are shown by dashed lines.

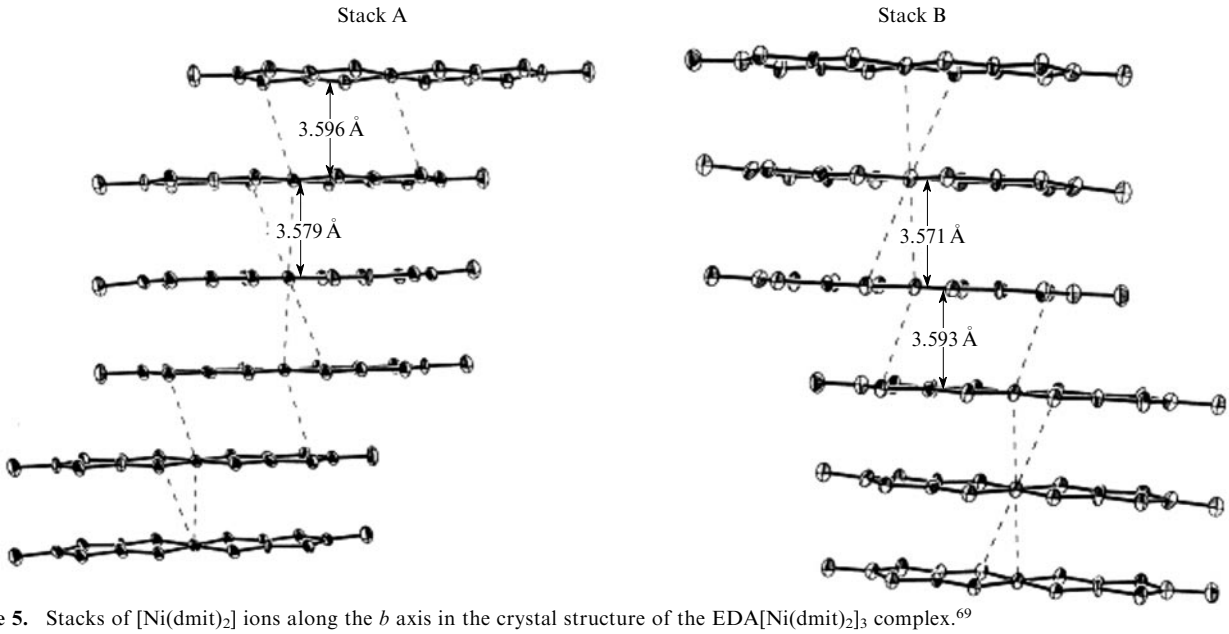


Figure 5. Stacks of $[Ni(dmit)_2]$ ions along the *b* axis in the crystal structure of the $EDA[Ni(dmit)_2]_3$ complex.[69]

above data, and this fact is also experimentally confirmed.[15, 65, 66]

According to the above data, cuprate complexes are more stable in the quasi-tetrahedral form. This fact is supported by experimental data.[67] Unlike nickelates, the stability of the quasi-tetrahedral structure even increases upon oxidation compared with the planar structure.

Finally, the mercurate complexes $[Hg(dmit)_2]^{n-}$ are much more stable in the quasi-tetrahedral form in both oxidation states, which is confirmed by available experimental data.[68]

An excellent analysis of different types of the crystal structures of dmit complexes is given in the review by Struchkov and co-workers.[51] The crystal structures of dmit complexes are governed by the ability of the planar $[M(dmit)_2]^{n-}$ ions to form stacks, which can be stabilized by S···S contacts shorter than the sum of the van der Waals radii. This imparts a certain two-dimensionality to the electronic structure of the crystals of dmit complexes, which distinguishes them from Krogmann complexes having essentially one-dimensional electrophysical and optical properties.[37] Figure 4 illustrates the structure of the $EDA[Ni(dmit)_2]_3$ complex (EDA is 2-diethylamino-1,3-dithiolanylium, $[Et_2NCS_2(CH_2)_2]^+$).[69]

Figure 5 shows the stacking motif of planar $[Ni(dmit)_2]$ complexes. In the stacks, there is an overlap between the $3d_z^2$ orbitals of nickel (Ni—Ni bonds are formed), which is similar to that between the $5d_z^2$ orbitals of platinum in Krogmann complexes,[37] as well as between the π orbitals characteristic of Bechgaard radical cation salts.[70]

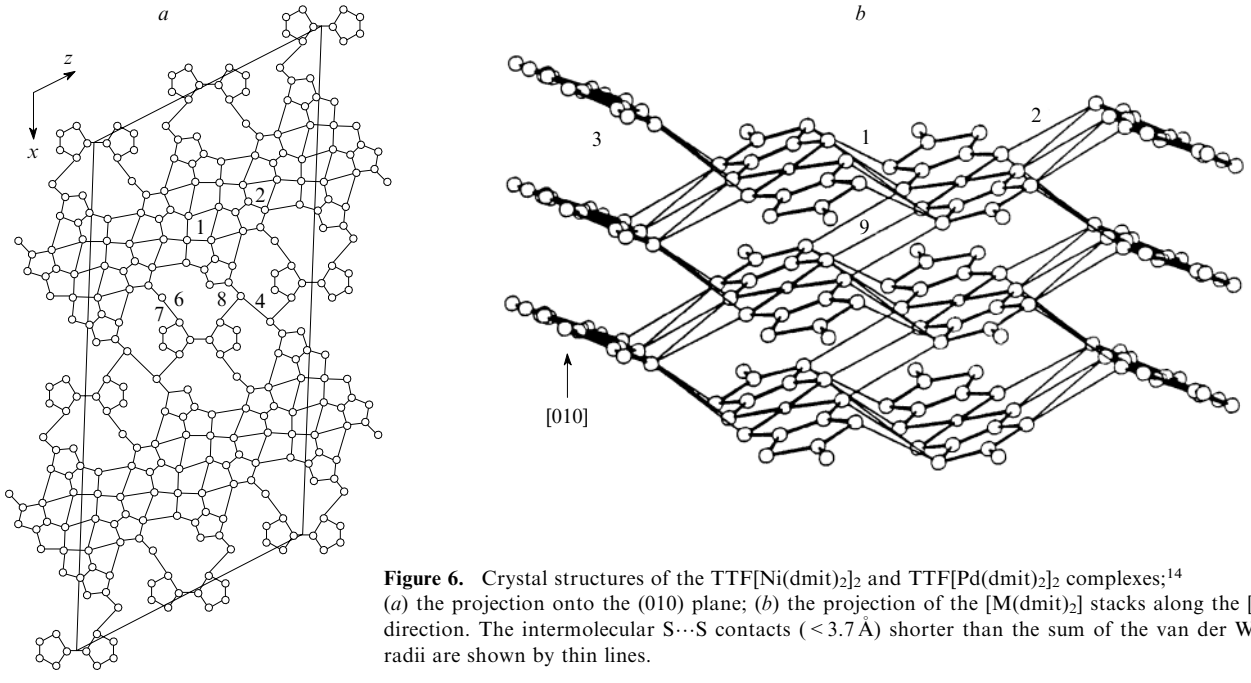


Figure 6. Crystal structures of the $TTF[Ni(dmit)_2]_2$ and $TTF[Pd(dmit)_2]_2$ complexes;[14] (*a*) the projection onto the (010) plane; (*b*) the projection of the $[M(dmit)_2]$ stacks along the [010] direction. The intermolecular S···S contacts (< 3.7 Å) shorter than the sum of the van der Waals radii are shown by thin lines.

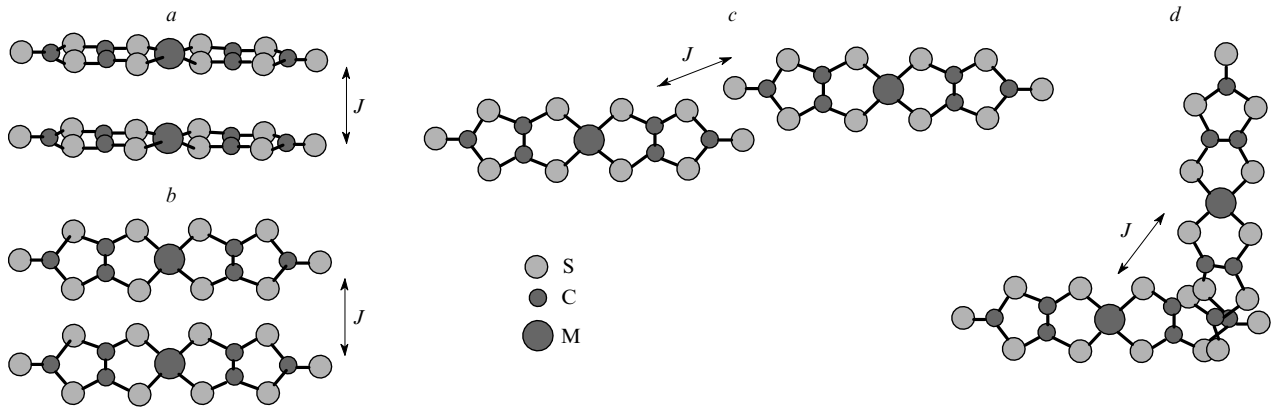


Figure 7. Different types of interactions (J) between $[M(dmit)_2]^{n-}$ ions;[71]
(a) the formation of π dimers; (b) side-by-side S···S interactions along the short axis of the ion; (c) side-by-side S···S interactions along the long axis of the ion; (d) orthogonal interactions between π orbitals.

As can be seen from Fig. 4, the structure of the $EDA[Ni(dmit)_2]_3$ complex is characterized by short contacts (compared with the sum of the van der Waals radii) between the thione sulfur atoms of the complex anions and the sulfur atoms of the cations. This imparts particular three-dimensional features to the electronic structure of the complex, resulting in the exchange interactions between anions along the long axis with the involvement of cations (indirect magnetic exchange). The quasi-three-dimensional structure for dmit complexes was found for the first time in the crystals of the superconducting $TTF[Ni(dmit)_2]_2$ complex and then in the $TTF[Pd(dmit)_2]_2$ complex (Fig. 6).[14]

Different types of interactions between the $[M(dmit)_2]^{n-}$ ions are shown in Fig. 7.

IV. Electrophysical properties of isotrithionedithiolate complexes

The close packing of $[M(dmit)_2]^{n-}$ ions facilitates the formation of a band, which is a conduction band in the case of a mixed valence (fraction value n). The close packing is possible in the case of small outer-sphere cations, as well as in the case of small n. Hence, the oxidation of $Ct_2[M(dmit)_2]$ complexes is accompanied by an increase in the overlap between orbitals of $[M(dmit)_2]^{n-}$ and a change in the electrophysical properties. For example, the $(Bu^n_4N)_2[Ni(dmit)_2]$ complex consists of the virtually isolated $[Ni(dmit)_2]^{2-}$ anions separated by large tetrabutylammonium cations and, consequently, has dielectric properties.[72] The oxidation of this complex with iodine affords the $Bu^n_4N[Ni(dmit)_2]$ complex, which crystallizes in two modifications: monoclinic[73] ($P2_1/c$) and triclinic[36] ($P\bar{1}$). The packing motifs of the $[Ni(dmit)_2]^-$ ions in these modifications are substantially different. In the monoclinic phase, there are stacks of $[Ni(dmit)_2]^-$ anions, but only weak S···S interactions are observed. On the contrary, in the triclinic phase, stacks are absent, but there are two types of S···S contacts (3.402 and 3.546 Å) substantially shorter than the sum of the van der Waals radii. Nevertheless, both complexes are poorly conducting: $\sigma_{rt} \approx 10^{-8}\ \Omega^{-1}\ cm^{-1}$ at room temperature.

The chemical oxidation of the $Bu^n_4N[Ni(dmit)_2]$ complex with bromine gives a poorly characterized conducting powder.[34] However, the electrochemical oxidation in a galvanostatic mode (in acetonitrile) affords well-faceted single crystals of the oxidation product.[34, 35] The composition of the complex was determined by elemental analysis, mass spectrometry and X-ray diffraction. According to these data, the complex has the formula $(Bu^n_4N)_{0.29}[Ni(dmit)_2]$. The electrical conductivity measured on single crystals by the Montgomery method is $10\ \Omega^{-1}\ cm^{-1}$ at 300 K. This is only slightly higher than the value determined with the use of powdered samples[74] ($1\ \Omega^{-1}\ cm^{-1}$). Usually, this difference is substantially larger due to the anisotropy and reflects the quasi-one-dimensional nature of most of synthetic metals. The temperature dependence of the electrical resistance is also unusual. Thus, in the temperature range of 300–158 K, the resistance changes according to the activation law with $E_a = 0.17$ eV, whereas $E_a = 0.05$ eV in the low-temperature range (158–77 K).

The factors responsible for these unusual electrophysical properties were revealed after the determination of the crystal structure and measurements of the resistance anisotropy in crystals. The $[Ni(dmit)_2]$ species are packed in stacks parallel to the b axis. There are contacts between the stacks shorter than the sum of the van der Waals radii of sulfur, resulting in the two-dimensional electronic structure. Therefore, the stacks are linked in layers parallel to the (001) plane; the layers are separated by $Bu^n_4N^+$ cations. According to measurements of the anisotropy, the electrical conductivities along the a and b axes are only slightly different ($\sigma_a/\sigma_b \approx 2$), whereas the electrical conductivity along the c axis is much lower, *i.e.*, $\sigma_a \approx \sigma_b \gg \sigma_c$.

Therefore, the $(Bu^n_4N)_{0.29}[Ni(dmit)_2]$ complex was the first example of conducting metal complexes of the quasi-two-dimensional nature. Synthetic metals of the quasi-two-dimensional nature have an advantage over quasi-one-dimensional metals. In accordance with the Peierls theorem,[75] the latter undergo the structural phase transition to the dielectric state. The period of the translation in the conducting one-dimensional stack increases by a factor of n, where $1/n$ is the population of the conduction band.[76] Quasi-two-dimensional metals also undergo the transition to the charge-density-wave state; however, the conducting state may be retained.

The neutral $[Ni(dmit)_2]$ complex has been described.[34] It was unexpectedly obtained as a by-product in the synthesis

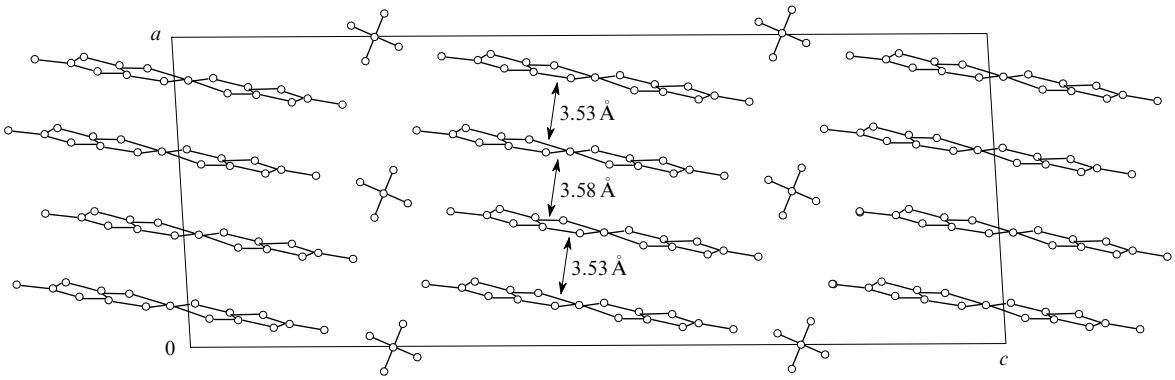


Figure 8. Crystal structure of the $(Me_4N)_{0.5}[Ni(dmit)_2]$ complex.[33]

of the superconducting $(TTF)_{0.5}[Ni(dmit)_2]$ complex. Crystals of the latter were obtained by the counter-diffusion of solutions of the $(TTF)_3[BF_4]_2$ salt and the $Bu^n_4N[Ni(dmit)_2]$ complex. It is interesting that the $TTF^{+\bullet}$ radical cation, being a weak oxidant [$E^\circ(TTF^{+\bullet}/TTF) = 0.33$ V with respect to the saturated calomel electrode], gives the fully oxidized complex, whereas the stronger oxidant bromine [$E^\circ(Br_2/Br^-) = 0.82$ V] gives the partially oxidized product.

In the crystals of the $[Ni(dmit)_2]$ complex, there are short contacts both in the stacks and between the stacks.[34]

Although the structure of the $[Ni(dmit)_2]$ complex meets the structural criteria for highly conducting systems (the close packing and short intermolecular interactions), one important criterion, *e.g.*, the mixed valence of the central atom, necessary for the partial population of the band is not fulfilled. Due to this fact, the $[Ni(dmit)_2]$ complex has low conductivity: $\sigma_{rt} = 10^{-3}\ \Omega^{-1}\ cm^{-1}$ at room temperature.

In the case of smaller outer-sphere cations, such as tetramethylammonium, the close contact between $[Ni(dmit)_2]$ is observed even for the composition $(Me_4N)_{0.5}[Ni(dmit)_2]$, and the latter complex exhibits metallic properties.[33] As follows from the stoichiometry of the complex, the population of the conduction band in this complex (formed by LUMO of the $[Ni(dmit)_2]$ complex) is 1/4 and, consequently, according to the Peierls theorem, the stacks of the planar $[Ni(dmit)_2]$ species should be tetramerized. This is actually observed:[33] almost planar $[Ni(dmit)_2]^{0.5-}$ anions form tetramerized stacks (Fig. 8). As can be seen from Fig. 8, the stacks consist of tetrads with two independent interplanar distances (3.53 and 3.58 Å). The stacks are linked by S···S contacts shorter than the sum of the van der Waals radii. Quantum chemical calculations confirmed the two-dimensional character of the conductivity of the crystals of the $(Me_4N)_{0.5}[Ni(dmit)_2]$ complex, which agrees with the data obtained from the analysis of the reflectance spectra.[77]

In spite of pronounced Peierls distortion, the complex has substantial electrical conductivity [in the (001) plane, $\sigma_{rt} \approx 50\ \Omega^{-1}\ cm^{-1}$], which increases on cooling down to ~ 10 K; at lower temperatures, the resistance becomes thermally activated. In the direction perpendicular to the (001) plane, the electrical conductivity is substantially lower ($\sim 10^{-2}\ \Omega^{-1}\ cm^{-1}$). Therefore, the anisotropy of the electrical conductivity is very large ($\sim 5 \times 10^3$) and, consequently, the $(Me_4N)_{0.5}[Ni(dmit)_2]$ complex can be assigned to quasi-two-dimensional synthetic metals. A relatively low pressure (~ 3 kbar) suppresses the transition to the dielectric phase at $T < 10$ K, and further cooling leads to the transition to the superconducting state, whose temperature increases with increasing pressure ($\partial T_C/\partial p > 0$) and reaches $T_C = 5$ K at 7 kbar (Fig. 9).

The related palladium complex $(Me_4N)_{0.5}[Pd(dmit)_2]$ crystallizes in two modifications, α and β (Fig. 10). The α phase is a semiconductor and does not undergo a transition to the superconducting state up to 12 kbar; the β phase is isomorphous with the crystals of the $(Me_4N)_{0.5}[Ni(dmit)_2]$ complex.[11] As can be seen from Fig. 10, $[Pd(dmit)_2]$ moieties form dyads in the stacks; the planes of the adjacent stacks separated by tetramethylammonium cations are parallel to each other, whereas these moieties form a corrugated surface in the crystals of the a phase. Compared with

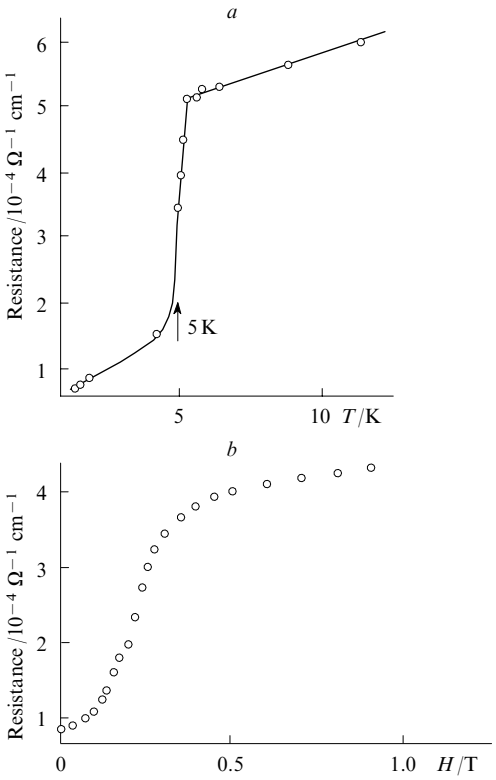


Figure 9. Transition to the superconducting state in the crystals of the $(Me_4N)_{0.5}[Ni(dmit)_2]$ complex at pressures of 7 kbar (*a*) and 3.2 kbar at 3 K (*b*).[33]

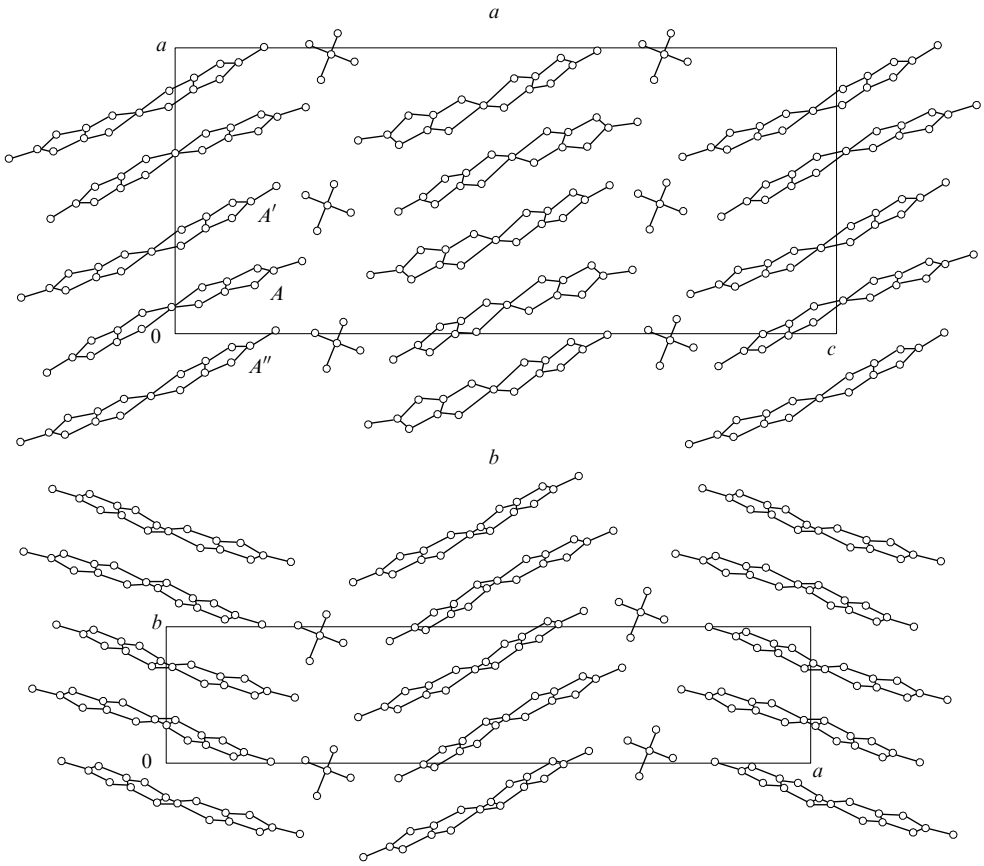


Figure 10. Crystal structures of β-$(Me_4N)_{0.5}[Pd(dmit)_2]$ (*a*) and α-$(Me_4N)_{0.5}[Pd(dmit)_2]$ (*b*).[11]

the $(Me_4N)_{0.5}[Ni(dmit)_2]$ complex, the stacks in the β-$(Me_4N)_{0.5}[Pd(dmit)_2]$ structure are dimerized to a more considerable degree; the interplanar distance in the dimer is 3.28 Å, whereas the distance between the dimers is 3.81 Å.[78] Taking into account the stoichiometry of the complex, it can be hypothesized that a decrease in the temperature should lead to the structural phase transition, resulting in the doubling of the period of the stack and the formation of tetrads (because the population of the conduction band is 1/4). This transitions was observed in the study.[78] In spite of the pronounced dimerization of the stacks, the β-$(Me_4N)_{0.5}[Pd(dmit)_2]$ complex has substantial electrical conductivity ($\sigma_{rt} \approx 33\ \Omega^{-1}\ cm^{-1}$) probably as a result of the two-dimensional character of the electronic structure due to S···S contacts between the stacks shorter than the sum of the van der Waals radii. After cooling to 200 K, the resistance of the crystals remains virtually unchanged, and then it sharply increases upon further decrease in the temperature (Fig. 11).

The resistance decreases with increasing pressure. As can be seen from Fig. 11, the dielectric–metal transition occurs at a pressure higher than 4 kbar. The temperature of this transitions (T_{MI}) rapidly decreases with increasing pressure. At a pressure higher than 6.5 kbar, only the transition to the superconducting state is observed.

Quantum chemical calculations by the DFT method[63] showed that there is a substantial difference between the $(Me_4N)_{0.5}[Ni(dmit)_2]$ and β-$(Me_4N)_{0.5}[Pd(dmit)_2]$ complexes. In the nickelate, the electronic states near the Fermi level are virtually one-dimensional and are produced mainly by LUMO of thee $[Ni(dmit)_2]$ molecules, whereas these states in the palladate are two-dimensional and produced from HOMO.

The investigation of other crystals of the composition $(Me_4E)_{0.5}[Pd(dmit)_2]$ (E = P, As, Sb) revealed the modified β structure, the so-called β′ structure.[78,79] These structures differ in the lattice parameter β and the tetrahedral anion site. Thus, the parameter β in the crystals of

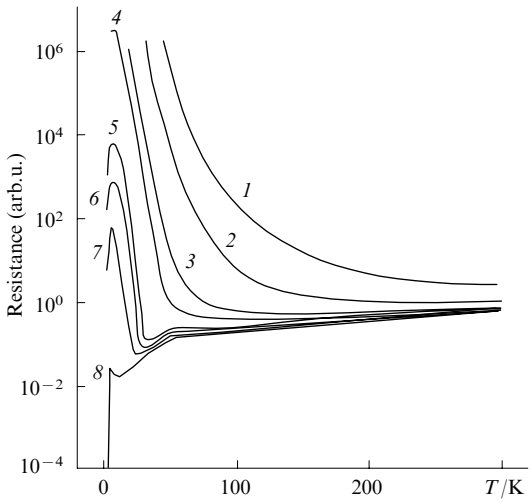


Figure 11. Temperature dependences of the resistance of the crystals of β-$(Me_4N)_{0.5}[Pd(dmit)_2]$ at different pressures (kbar): 0.001 (*1*), 2.2 (*2*), 4.2 (*3*), 4.8 (*4*), 5.3 (*5*), 5.5 (*6*), 5.8 (*7*), 6.3 (*8*).[78]

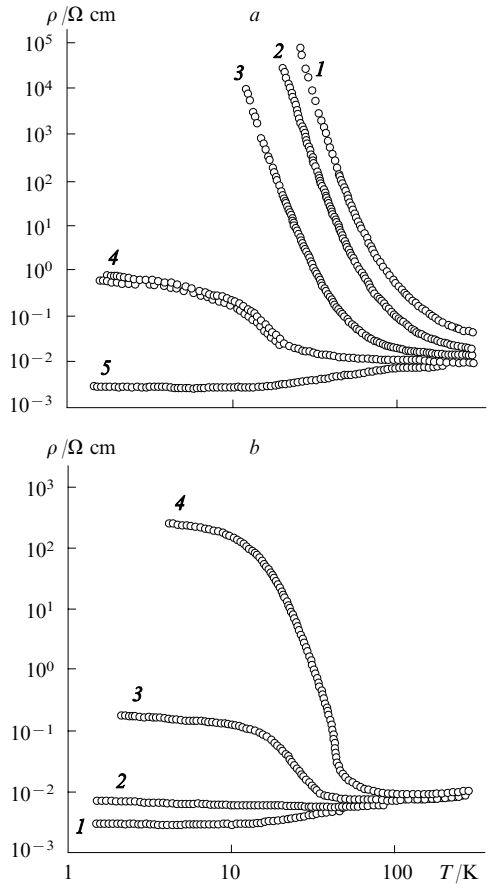


Figure 12. Temperature dependences of the resistance of the crystals of β′-$(Me_4Sb)_{0.5}$[Pd(dmit)$_2$] at different pressures (kbar);[78]
(*a*): 0.001 (*1*), 3.4 (*2*), 6.1 (*3*), 7.9 (*4*), 9.7 (*5*);
(*b*): 9.7 (*1*), 11.5 (*2*), 11.9 (*3*), 13.2 (*4*).

β-$(Me_4N)_{0.5}$[Pd(dmit)$_2$] and β′-$(Me_4As)_{0.5}$[Pd(dmit)$_2$] is 90.94° and 97.85°, respectively.[11] In the crystals of the β′ phases, the interplanar distances in the dimer are larger, whereas the distances between the dimers are smaller. For instance, these distances in the β′-$(Me_4P)_{0.5}$[Pd(dmit)$_2$] complex are 3.72 and 3.32 Å, respectively.[11]

Under atmospheric pressure, all β′-$(Me_4E)_{0.5}$[Pd(dmit)$_2$] complexes are semiconductors.[78] The β′-$(Me_4P)_{0.5}$.[Pd(dmit)$_2$] and β′-$(Me_4As)_{0.5}$[Pd(dmit)$_2$] complexes retain semiconducting properties up to 15 and 17.3 kbar, respectively. The unusual influence of the pressure on the temperature dependence of the resistance was observed for the β′-$(Me_4Sb)_{0.5}$[Pd(dmit)$_2$] complex (Fig. 12). Under atmospheric pressure, the complex is a narrow-band semiconductor (E_a = 0.05 eV). At a pressure of ~10 kbar, it exhibits metallic properties, but the superconductivity is absent down to 1.5 K. A further increase in the pressure again leads to the semiconducting state. Therefore, the effect of the pressure on the electrophysical properties of the complexes of the β′ phase depends on the nature of the E atom in the outer-sphere cation. This dependence is non-monotonic: the complex with the smallest $(Me_4N)^+$ cation goes to the superconducting state under high pressure, whereas complexes with larger cations do not undergo this transition.

More recently, it was found[80] that the pressure has an unusual effect on the electrophysical properties of the crystals of the β′-$(Me_4E)_{0.5}$[Pd(dmit)$_2$] complexes. For example, the uniaxial pressure along the crystallographic axis *b* rapidly suppresses the dielectric phase of β′-$(Me_4As)_{0.5}$[Pd(dmit)$_2$], and the complex goes to the superconducting state with T_C = 4 K even at 7 kbar. On the contrary, the uniaxial pressure up to 2 kbar along the crystallographic axes *a* or *c* stabilizes the dielectric phase. This unusual behaviour is indicative of the crucial role of interactions in and between the dimers, because they have an effect on the band width and the efficient single-site Coulomb interaction.

To summarize, the following important features of palladate complexes may be highlighted:

1) the energy difference between LUMO and HOMO in the [Pd(dmit)$_2$] molecule is small;

2) in the crystals of the complexes, the stacks of [Pd(dmit)$_2$] are substantially dimerized;

3) intermolecular interactions with the participation of HOMO are predominantly two-dimensional, whereas interactions with the participation of LUMO are one-dimensional due to the difference in the symmetry of these orbitals.

Quantum chemical calculations of the overlap integrals between LUMO and HOMO were carried out.[78] In Table 4 these integrals are denoted as H−H (LUMO−LUMO), B−B and H−B, respectively. The overlap integrals in the dimers (*A*), between the dimers (*B*) (see Table 4), as well as between adjacent stacks (Fig. 13) are given.

By comparing the values of *A* and *B*, it can be concluded that the degree of dimerization in the stacks of [Pd(dmit)$_2$] systematically changes with a change in the size of the outer-sphere cation, the degree of dimerization being favourable for the stability of the metal phase under high pressure. It should be noted that the reverse situation is observed for bis(ethylenedithio)tetrathiafulvalene (ET)-based radical cation salts: an increase in the degree of dimerization gives rise to a dielectric state.[81]

By assuming the model of dimerized stacks in the [Pd(dmit)$_2$] complexes, the following three parameters are

Table 4. Intermolecular overlap integrals ($\times 10^3$) for the frontier orbitals of $(Me_4E)_{0.5}$[Pd(dmit)$_2$] complexes.[78]

Overlap integral	E = N			E = P			Overlap integral	E = As			E = Sb		
	H−H	B−B	H−B	H−H	B−B	H−B		H−H	B−B	H−B	H−H	B−B	H−B
A	41.86	−43.92	−0.94	40.97	−44.78	−0.10	*A*	41.05	−44.88	−0.85	41.29	−44.84	−1.24
B	−1.92	−5.35	−0.88	−3.50	−7.11	−1.90	*B*	−3.29	−6.78	−1.97	−2.65	−5.91	−1.51
p	1.00	−2.37	−0.71	1.24	−3.10	−0.81	*p*	1.24	−2.96	−0.88	1.00	−2.36	−0.69
q_1	−0.82	−2.01	−0.41	−0.95	−1.75	−0.38	q_1	−0.86	−1.77	−0.31	−0.74	−1.64	−0.28
q_2	−0.82	−2.01	0.61	−0.95	−1.75	0.58	q_2	−0.86	−1.77	0.55	−0.74	−1.64	0.54
r	1.76	−4.90	−1.44	1.92	−4.34	−1.23	*r*	2.03	−4.60	−1.27	2.05	−4.92	−1.34

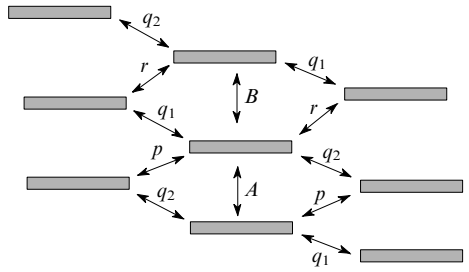


Figure 13. Calculation scheme of the overlap integrals in the crystals of β′-$(Me_4E)_{0.5}$[Pd(dmit)$_2$] complexes (E = N, P, As, Sb).

sufficient for the interpretation of their optical properties: the transfer integrals t_1 and t_2 between HOMO and LUMO, respectively, and the energy difference ΔE between HOMO and LUMO. In this case we obtain two types of energy diagrams for these complexes shown in Fig. 14.

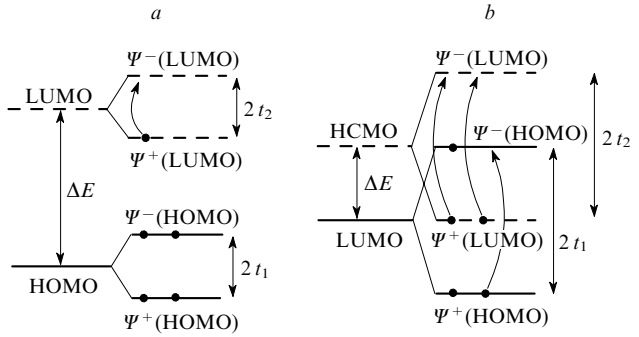


Figure 14. Two types of the energy diagrams for $Ct_{0.5}$[Pd(dmit)$_2$] complexes;[82]
(*a*) case 1: $\Delta E > t_1 + t_2$; (*b*) case 2: $\Delta E < t_1 + t_2$.

The scheme presented in Fig. 14*a* is observed in most cases; the scheme shown in Fig. 14*b* was found in the $Cs_{0.5}$[Pd(dmit)$_2$] complex.[82] The excitation energies and the intensities of transitions (I_σ) are described by the following expressions:

case 1 (Fig. 14*a*):

Ψ^+(LUMO) $\longrightarrow$ Ψ^-(LUMO):

$$\hbar\omega_0 = 2t_2,$$

$$I_\sigma = \frac{4\pi e^2 d^2 t_2}{V\hbar^2};$$

case 2 (Fig. 14*b*):

Ψ^+(HOMO) $\longrightarrow$ Ψ^-(HOMO):

$$\hbar\omega_0 = 2t_1,$$

$$I_\sigma = \frac{4\pi e^2 d^2 t_1}{V\hbar^2},$$

C^+(LUMO) $\longrightarrow$ C^-(LUMO):

$$\hbar\omega_0 = 2t_2;$$

$$I_\sigma = \frac{8\pi e^2 d^2 t_2}{V\hbar^2},$$

where $\hbar$ is Planck's constant, ω_0 is the circular frequency of absorption in the frozen orbital approximation, e is the charge of the electron, V and d are the volume of the dimer and the interplanar distance in the dimer, respectively.

The complexes of the composition $(Me_3EtN)_{0.5}$[Pd(dmit)$_2$] and $(Et_4N)_{0.5}$[Pd(dmit)$_2$] were characterized.[83] Both complexes belong to narrow-band semiconductors; the electrical conductivity of the former complex ($\sigma_{rt} = 58\ \Omega^{-1}\ cm^{-1}$) is substantially higher than that of the latter ($\sigma_{rt} = 2.2\ \Omega^{-1}\ cm^{-1}$).The band gap width in the former complex is 0.056 eV in the range of 300–80 K and 0.02 eV in the low-temperature range; the band gap width in the latter complex is 0.036 eV in the range of 300–45 K. In the study,[83] the superconductivity was not observed; however, it would be possible for the $(Me_3EtN)_{0.5}$[Pd(dmit)$_2$] complex under high pressure because the size of the Me_3EtN^+ cation is intermediate between the sizes of the Me_4N^+ and $Me_2Et_2N^+$ cations. Both complexes with these cations are superconductors. The α-$(Me_4N)_{0.5}$[Pd(dmit)$_2$] complex becomes a superconductor at $T_C = 6.2$ K and $p = 6.5 \times 10^8$ Pa; $(Me_2Et_2N)_{0.5}$[Pd(dmit)$_2$], at $T_C = 4$ K and $p = 2.4 \times 10^8$ Pa.

The complex of the composition $(Ph_4P)_{1/3}$[Ni(dmit)$_2$] has a peculiar crystal structure[84] (Fig. 15). The [Ni(dmit)$_2$]

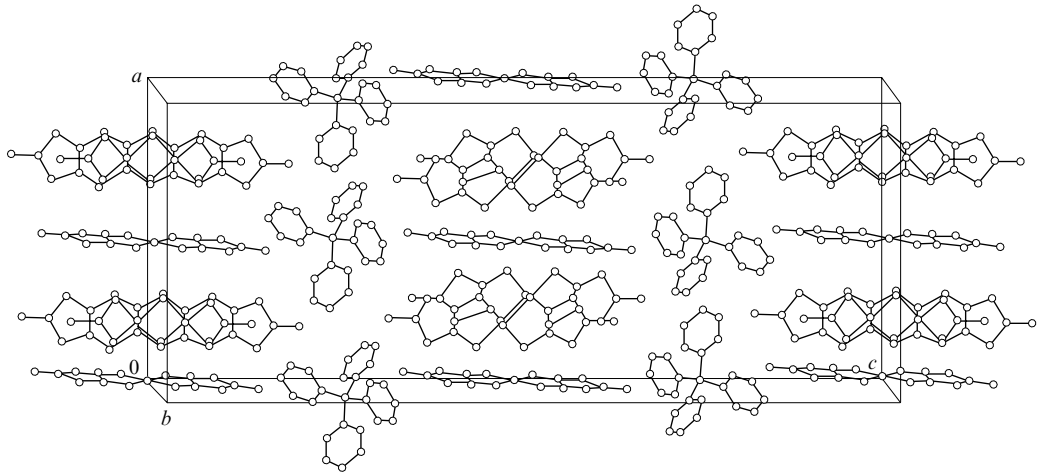


Figure 15. Crystal structure of the $(Ph_4P)_{1/3}$[Ni(dmit)$_2$] complex.[84]

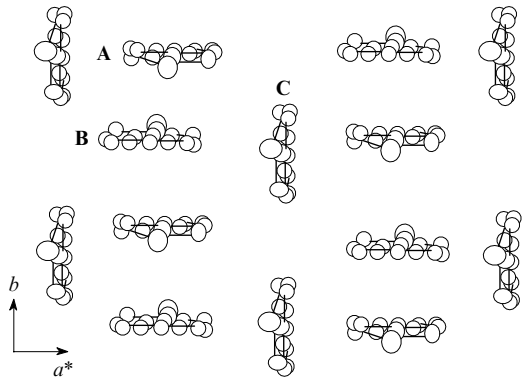
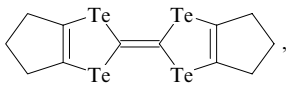


Figure 16. Packing of $[Ni(dmit)_2]$ anions along the *c* axis in the crystals of the $(Ph_4P)_{1/3}[Ni(dmit)_2]$ complex.[84]

moieties are packed in an usual fashion. Two of them form stacks along the [010] direction (molecules **A** and **B**, Fig. 16), whereas the third $[Ni(dmit)_2]$ moiety is located perpendicular to these stacks (molecule **C** in Fig. 16) and separates the dimerized stacks. Such structures are very rare. A similar structure was found for the radical cation salt $(HMTTeF)_4(PF_6)_2$ (HMTTeF is hexamethylenetetratellurafulvalene) [85]



HMTTeF

and the radical anion salt (*N*-Etpyz)$(TCNQ)_{2.5}$ (pyz is pyrazine) synthesized in our study.[86]

The electrical conductivity of the crystals of the $(Ph_4P)_{1/3}[Ni(dmit)_2]$ complex along the *b* axis (the direction of the stacks) at room temperature is 10 Ω^{-1} cm^{-1}, and it exhibits the semiconductor type of the temperature dependence; the anisotropy of the conductivity $\sigma_b/\sigma_{a^*} = 100$. The activation energy for the conductivity is 0.046 eV in the range from room temperature to 125 K; at $T < 125$ K, the activation energy is 0.035 eV. The change in the activation energy near 125 K is attributed to the anion ordering.[84] The $(Ph_4As)_{1/4}[Ni(dmit)_2]$ complex has similar properties.[87] At 60 K, the temperature dependence of the electrical resistance of this complex shows an effect associated with a decrease in the dielectric gap width from 0.03 to 0.01 eV.

The related palladium complex $(Ph_4P)_{1/3}[Pd(dmit)_2]$ (see Ref. 88) is structurally similar to $(MePh_3P)_{1/3}[Pd(dmit)_2]$ (Fig. 17). As can be seen from Fig. 17, the structure is formed by stacks of $[Pd(dmit)_2]$ separated by stacks of isolated $MePh_3P^+$ cations. In turn, the stacks of $[Pd(dmit)_2]$ consist of dimers formed *via* strong Pd···Pd interactions (Fig. 18, solid lines). In addition, there are side-by-side S···S contacts shorter than the sum of the van der Waals radii. The $[Pd(dmit)_2]_2$ dimers are packed along the *c* axis. In the $(MePh_3P)_{1/3}[Pd(dmit)_2]$ complex, all $[Pd(dmit)_2]$ moieties are dimerized, whereas only half of the moieties are dimerized in the related nickel complex.[87]

The Pd···Pd distances in the crystals of the $(MePh_3P)_{1/3}.[Pd(dmit)_2]$ complex are in the range of 2.9194 – 3.0956 Å, which is only slightly larger than the sum of the crystal-chemical radii of palladium (2.74 – 2.75 Å).[89,90] As can be

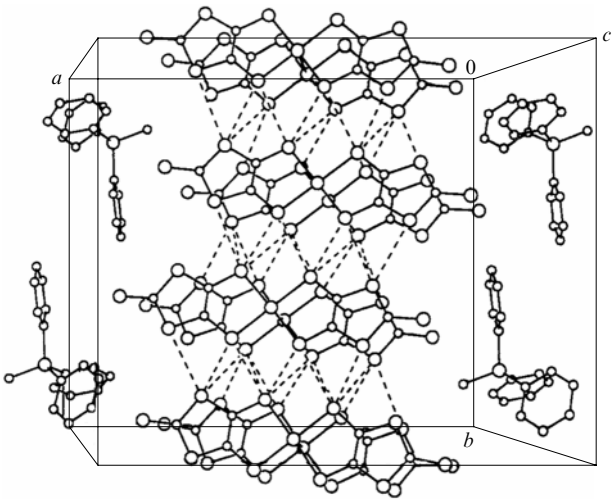


Figure 17. Crystal structure of the $(MePh_3P)_{1/3}[Pd(dmit)_2]$ complex.[88] The stacks of $[Pd(dmit)_2]$ are separated by columns of $MePh_3P^+$ cations.

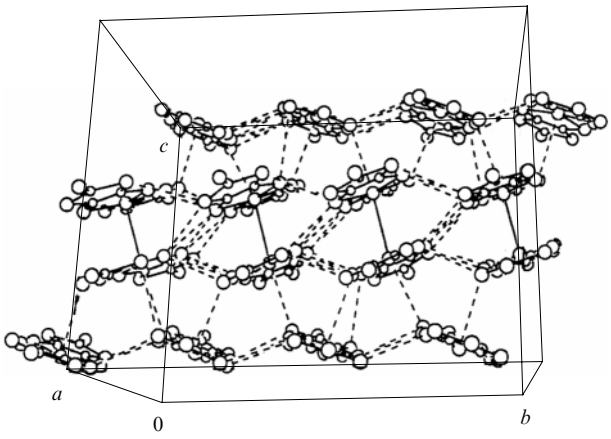


Figure 18. Packing of the $[Pd(dmit)_2]_2$ dimers along the *c* axis in the crystals of the $(MePh_3P)_{1/3}[Pd(dmit)_2]$ complex.[88]
The S···S and Pd···S contacts shorter than the sum of the van der Waals radii are shown by dashed lines.

seen from Fig. 18, each dimer is linked to six adjacent dimers by short S···S interactions to form a two-dimensional layer. These contacts vary from 3.327 Å (the shortest distance) to 3.665 Å (the longest distance shown in Fig. 18 as dashed lines). These distances are much smaller than the sum of the van der Waals radii of sulfur (3.70 Å).[91]

Due to a substantial two-dimensionality of the electronic system, complexes of the composition $(R_4E)_{1/3}.[Pd(dmit)_2]$ are narrow-band semiconductors (Table 5).

The $(Etpy)_{0.5}[Ni(dmit)_2]$ complex (Etpy is *N*-ethylpyridinium) is a two-dimensional metal.[92] The $[Ni(dmit)_2]^{-0.5}$ anions form stacks, which are linked together by S···S contacts shorter than the sum of the van der Waals radii (Fig. 19). The complex exhibits metallic properties in the range of 282 – 269 K; the metal – dielectric transition occurs at temperatures below 269 K. When heated above 282 K, the complex also exhibits dielectric properties, the temperature dependence of the resistance $[\rho(T)]$ being reproduced in the cooling – heating mode. The IR spectra show a

Table 5. Specific electrical conductivities at room temperature and the band gap widths (Δ) for $(R_4E)_{1/3}[M(dmit)_2]$ complexes.[88]

Complex [a]	σ_{rt} /Ω^{-1} cm^{-1}	Δ /meV
$(MePh_3P)_{1/3}[Pd(dmit)_2]$	13	100
$(Ph_4P)_{1/3}[Pd(dmit)_2]$	1	55
$(MePh_3P)_{1/3}[Ni(dmit)_2]$	0.1	220
$(Ph_4P)_{1/3}[Ni(dmit)_2]$	10	17
$(BTP)_{1/3}[Pd(dmit)_2]$	80	—
$(PPN)_{1/3}[Pd(dmit)_2]$	62	50
$(BTP)_{1/3}[Ni(dmit)_2]$	0.2	—
$(PPN)_{1/3}[Ni(dmit)_2]$	45	—

[a] BTP is benzyltriphenylphosphonium, PPN is bis(triphenylphosphoranylidene)ammonium.

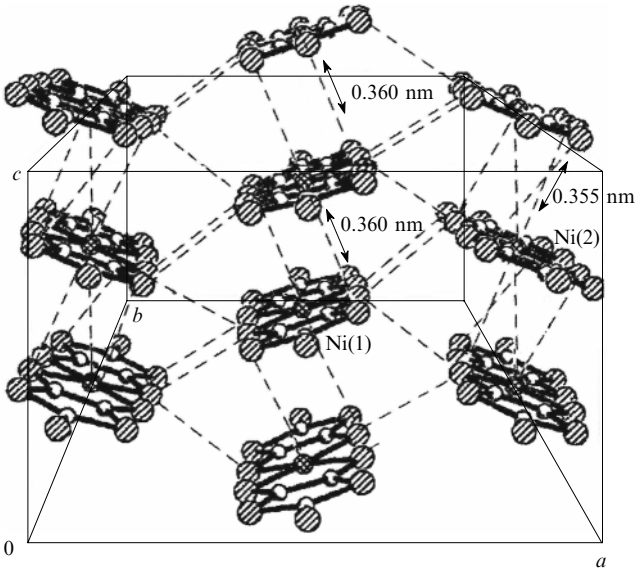


Figure 19. Two-dimensional conducting layers in the crystals of the $(Etpy)_{0.5}[Ni(dmit)_2]$ complex.[92]
The intermolecular contacts shorter than the sum of the van der Waals radii are shown by dashed lines.

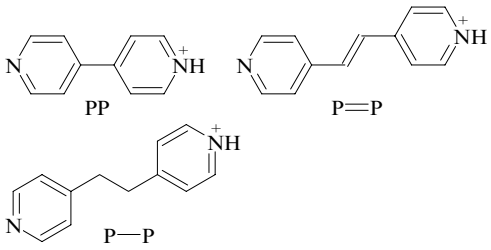
decrease in the vibrational frequencies ν(C=C) and ν(C=S) upon oxidation of the starting Etpy[Ni(dmit)$_2$] complex. The vibrational frequency ν(C=C) in the starting complex is 1347 cm^{-1}, whereas the spectrum of the oxidized complex shows a doublet at 1331 and 1237 cm^{-1}; the vibrational frequency ν(C=S) decreases after oxidation from 1050 to 1041 cm^{-1}. In the study,[92] the splitting of the spectral line belonging to vibrations of the C=C bonds was attributed to the disproportionation of the complex having a semi-integer charge into the neutral and monoanionic complexes:

$$2\,[Ni(dmit)_2]^{0.5-} \rightleftharpoons [Ni(dmit)_2] + [Ni(dmit)_2]^{-}.$$

Taking into account the characteristic time of vibrational spectroscopy (10^{-11} s),[93] it should be noted that this interpretation implies that the rate constant of disproportionation is at most 10^{11} s^{-1}.

In the above-mentioned EDA[Ni(dmit)$_2$]$_3$ complex (see Fig. 5), the anisotropy of the electrical resistance is $\sigma_a : \sigma_b : \sigma_c = 1 : 2 : 10^{-4}$ (see Ref. 69). The electrical conductivity along the b axis at room temperature $\sigma_b = 0.2\ \Omega^{-1}$ cm^{-1} is thermally activated with the activation energy of 0.11 eV.

Interesting structures are observed in the crystals of salts containing cations capable of forming hydrogen bonds. For example, 1 : 1 complexes with the following cations were described:[94]



In the crystals of the $(PP)_2[Ni(dmit)_2]_2 \cdot TCE$ complex (TCE is 1,1,2-trichloroethane), the PP cations form one-dimensional chains *via* NH···N hydrogen bonds. The $[Ni(dmit)_2]^-$ anions are dimerized (plane-to-plane overlap); the interplanar distance is 3.69 Å. These dimers are located between the chains of PP cations, thus forming a sandwich structure (Fig. 20).

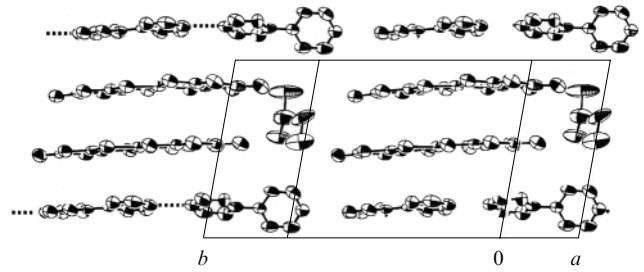


Figure 20. The arrangement of the ions in the crystal structure of $(PP)_2[Ni(dmit)_2]_2 \cdot TCE$.[94]

The $(P{=}P)_2[Ni(dmit)_2]_2 \cdot PhCl$ and $(P{-}P)[Ni(dmit)_2]$ complexes also have similar structures; however, the $[Ni(dmit)_2]^-$ anions in the latter case do not form dimers. In spite of the similarity of the crystal and electronic structures, the electrophysical properties of the complex with the PP cation substantially differ from the properties of the complexes with the P=P and P−P cations. The latter two complexes are semiconductors with the band gap width of 0.21–0.25 eV, which is characteristic of dmit complexes with singly charged anions; the electrical conductivity of the $(PP)_2[Ni(dmit)_2]_2 \cdot TCE$ complex is much higher, and the temperature dependence of the electrical resistance is described by the expression

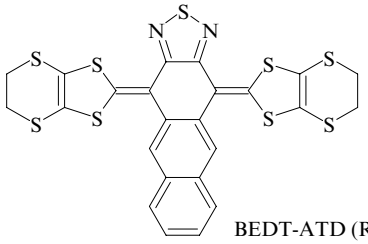
$$\frac{\rho(T)}{\rho(295\,K)} = AT^{-\alpha}\exp\left(-\frac{\Delta}{kT}\right)$$

with the parameters $\alpha = 1.6$, $\Delta/k = 353$ K. It is known[95] that this dependence is characteristic of semiconductors, in which the carrier mobility and concentration are proportional to $T^{-\alpha}$ and $\exp(-\Delta/kT)$, respectively. In this case, the band gap width is unusually small (0.03 eV), whereas this parameter in two other complexes is 7–8 times larger.

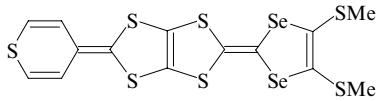
In the study,[92] this fact was attributed to the presence of the n-donor level, whose nature is, however, unknown.

Similar complexes with hydrogen bonds were described.[96] These are complexes with the singly charged $[Ni(dmit)_2]^-$ anions and 2-, 3- and 4-methoxycarbonyl-*N*-methylpyridinium cations (2-MMP, 3-MMP and 4-MMP, respectively). In the crystals of all the above-mentioned complexes, the cations and anions form sandwich structures, in which the anions are located between the layers or dimers of the cations. Weak hydrogen bonds are formed between the hydrogen atoms of the pyridine rings and the methyl group and the carboxy groups of adjacent cations. According to the structure and stoichiometry of the complexes, they belong to high-ohmic semiconductors; their specific electrical conductivities are 4.33×10^{-10}, 1.80×10^{-6} and $5.60 \times 10^{-6}\ \Omega^{-1}\ cm^{-1}$ for the (2-MMP).[Ni(dmit)$_2$], (3-MMP)[Ni(dmit)$_2$] and (4-MMP)[Ni(dmit)$_2$] complexes, respectively.[96]

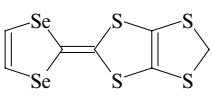
First organic metals and superconductors were synthesized based on planar symmetrical molecules (symmetry not lower than D_{2h}). In the late 1990s, organic metals and superconductors based on unsymmetrical polyheterocyclic organic compounds were prepared. The structures of these compounds are shown below.



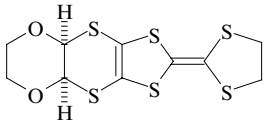
BEDT-ATD (Ref. 97)



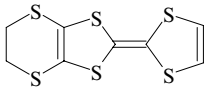
TM-TPDS (Ref. 98)



MDT-TSF (Ref. 99)

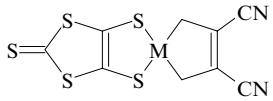


DODHT (Ref. 100)



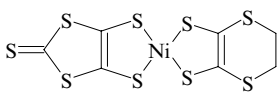
EDT-TTF (Ref. 101)

Unsymmetrical dithiolate complexes based on dmit were synthesized, and some of them exhibit metallic properties.[102]

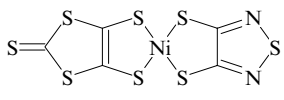


[M(dmit)(mnt)]

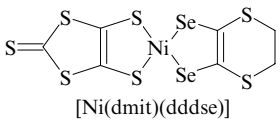
M = Ni, Pd, Pt.



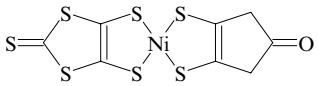
[Ni(dmit)(dddt)]



[Ni(dmit)(tdas)]



[Ni(dmit)(dddse)]



[Ni(dmit)(dmio)]

All complexes with $[Ni(dmit)(mnt)]^{n-}$ anions are highly conducting (Fig. 21). As can be seen from Fig. 21, the TTF[Ni(dmit)(mnt)] and α-(EDT-TTF)[Ni(dmit)(mnt)] complexes exhibit metallic properties down to 30 K; at lower temperatures, the metal–dielectric transition occurs.

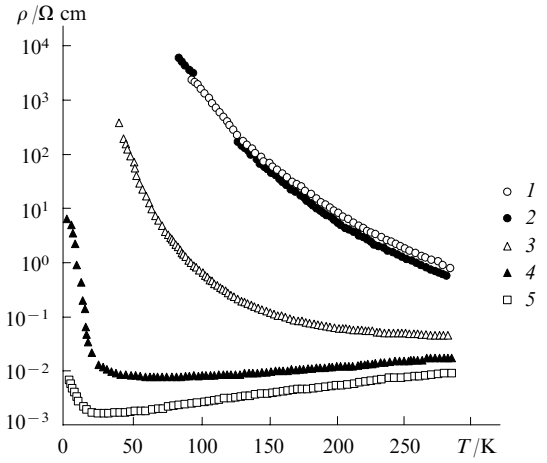


Figure 21. Temperature dependences of the electrical resistance of the crystals of complexes with [Ni(dmit)(mnt)] anions.[102]
The cations: $Me_2Et_2N^+$ (*1*), Me_4N^+ (*2*), BPDT-TSeF (*3*), TTF (*4*), and EDT-TTF (α phase of the complex) (*5*). BPDT-TSeF is bis(propylenedithio)tetraselenafulvalene.

Figure 22 shows the temperature dependences of the electrical resistance of the TTF[Ni(dmit)(tdas)] and (EDT-TTF)[Ni(dmit)(tdas)] complexes. Both complexes exhibit metallic properties. It should be noted that the TTF.[Ni(dmit)(tdas)] complex retains metallic properties down to 4 K. The (EDT-TTF)[Ni(dmit)(tdas)] complex forms two crystalline phases (α and β). Crystals of the α phase exhibit metallic properties, whereas crystals of the β phase have dielectric properties. The X-ray diffraction study showed

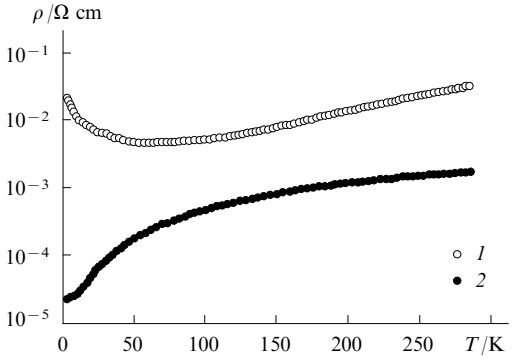


Figure 22. Temperature dependences of the electrical resistance of complexes with [Ni(dmit)(tdas)] anions.[102]
The cations: EDT-TTF (*1*), TTF (*2*).

that the crystals of α-(EDT-TTF)[Ni(dmit)(tdas)] are isostructural with the crystals of the α-(EDT-TTF)[Ni(dmit)$_2$] complex, which is a superconductor with T_C = 1.3 K under normal pressure.[102]

V. Magnetic properties of isotrithionedithiolate complexes

The specific features of the crystal structures of dmit complexes (overlap of p orbitals of planar [M(dmit)$_2$] complexes in the stacks, the M ← S coordination bonds between adjacent molecules, S···S distances shorter than the sum of the van der Waals radii) may not only be responsible for the electrical conductivity of the material but also lead to the formation of magnetically ordered structures, *viz*., chain and two-dimensional antiferromagnets, as well as spin ladders.

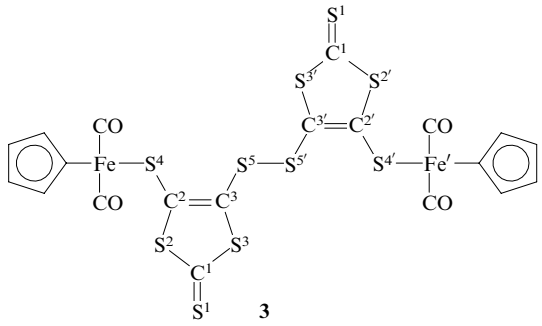
We synthesized and studied the Bu^n_4N[Pt(dmit)$_2$] complex[40] and showed that the stacks of anions characteristic of most of dmit complexes are absent in this complex. Instead, the crystal structure of this complex contains zigzag ribbons, in which there are short S···S contacts between adjacent anions.[40]

The existence of this quasi-one-dimensional chain could be favourable for the conductivity along the chain. However, the electrical conductivity measured on single crystals is at most 10^{-8} Ω^{-1} cm^{-1}, which is characteristic of dmit complexes with singly charged [M(dmit)$_2$]$^-$ anions. Nevertheless, the indirect antiferromagnetic exchange between Pt^{III} ions may occur along the chain. This exchange was actually found.[39] The Bu^n_4N[Pt(dmit)$_2$] complex is paramagnetic; the magnetic susceptibility (χ) obeys the Curie–Weiss law in the range of 300–4.2 K with the temperature-independent paramagnetic term (Van Vleck paramagnetism):

$$\chi(T) = \chi_0 + \frac{C}{T-\theta},$$

$\chi_0 = 1.18 \times 10^{-3}$ mol^{-1}, the Curie constant C = 0.310 K mol^{-1}, the Weiss constant $\theta = -26.3$ K. According to EPR measurements,[38] the spins in this complex are localized at the platinum atoms. Hence, the large value of the Weiss constant indicates that the interaction along the Pt–S···S–Pt chain is rather strong.

Another unusual example of interactions between spins along an unconjugated chain was found[103] in the dinuclear iron(II) complex **3**, whose molecule has C_2 symmetry.



3

The point symmetry group of this complex (C_2) contains only one-dimensional irreducible representations (A and B). Hence, all its electronic and nuclear states should be non-degenerate. The removal of the degeneracy is possible only due to interactions between electrons along the Fe–S(4)–C(2)–C(3)–S(5)–S(5′)–C(3′)–C(2)–S(4′)–Fe′ chain. In the Mössbauer spectrum, these interactions appear as two quadrupole doublets with almost equal isomer shifts but with substantially different values of the quadrupole coupling: Δ_1(300 K) = 1.09, Δ_2(300 K) = 0.64 mm s^{-1} (Ref. 103). The larger value is associated with the contribution of the electronic states of B symmetry to the electric field gradient on the nucleus; the smaller value, with the contribution of the states of A symmetry. These interactions are responsible for the paramagnetism of the complex. Thus, the temperature dependence of the magnetic susceptibility obeys the Curie–Weiss law with the Weiss constant $\theta = -6.5$ K. Taking into account a considerable length of the chain that links two iron atoms, this Weiss constant should be considered as large. The effective magnetic moment (3.13 μ_B) calculated from the Curie constant corresponds to two unpaired electrons, which is also an unusual fact. For Fe^{2+} ions with the $3d^6$ electron configuration, the diamagnetic ground state would be expected in the field of a strong-field ligand (cyclopentadienyl anion, CO molecules). In the case of paramagnetism, the number of unpaired electrons should be at least 4 (electrons at each site pair up). Hence, the paramagnetism of this dinuclear complex is apparently attributed to the triplet ground state with the delocalized spin density.

This hypothesis was confirmed by quantum chemical calculations at the RODFT level of theory with the B3LYP/6-31(dp)G basis set.[103] The triplet ground state is separated from the excited singlet state by a gap of 1.5 eV, and the spin density is essentially delocalized (Fig. 23).

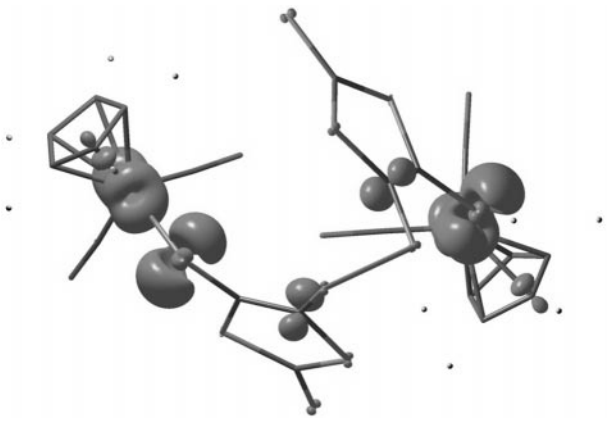


Figure 23. Spin density distribution in the molecule of complex **3**.[103]

It should be emphasized that the splitting of degenerate electronic states in a low-symmetry molecule discovered in our studies is analogous to the so-called Davydov (exciton) splitting in crystals, whose unit cells contain Z molecules.[104]

A comprehensive review of the magnetic properties of dmit-based complexes, including complexes with outer-sphere metallocenium cations, was given in the study.[105] Hence, we restrict ourselves to the analysis of studies published in the last eight years.

Two polymorphs of the complex with a supramolecular cation, *viz*., the anilinium cation intercalated into 18-crown-6, [(PhH_3N^+)⊂(18-crown-6)][Ni(dmit)$_2$] (**4**), were described.[106] In the crystals of these phases, the [Ni(dmit)$_2$]$^-$ anions are linked together to form dimers, which, in turn, form chains separated by supramolecular cations. In the

crystals of the α phase, the supramolecular cations form regular stacks, resulting in the formation of a spin-ladder structure by the $[Ni(dmit)_2]_2^{2-}$ dimers.

In the authors' opinion,[106] this is supported by the fact that the temperature dependence of the magnetic susceptibility is best described by a spin-ladder model (α is the model parameter) proposed in the study:[107]

$$\chi_{ladder} = \frac{\alpha}{\sqrt{T}} \exp\left(-\frac{\Delta_\chi}{kT}\right)$$

with the spin gap $\Delta_\chi = 190$ K. It should be noted that, according to the study,[21] the formula for the temperature dependence of the magnetic susceptibility of a spin ladder takes another form:

$$\chi_{ladder} = \frac{c_1}{T}\left[1 + \left(\frac{T}{c_2}\right)^{c_3}\left(e^{c_4/T} - 1\right)\right]^{-1}\left[1 + \left(\frac{c_5}{T}\right)^{c_6}\right]^{-1},$$

where $c_1 - c_6$ are the fitting parameters.

To support this interpretation, the authors of the study [106] calculated the transfer integrals by the extended Hückel method. The strongest interaction was observed along the ladder steps (the transfer integral $t_\perp = 45.3$ meV); along the ladder rungs, $t_{||} = 15.9$ meV.[106]

The crystal density of the β phase is 3% higher than that of the α phase. The supramolecular packing of the cations is distorted. This hinders intermolecular interactions between the $[Ni(dmit)_2]_2^{2-}$ dimers along the ladder rungs, which is observed in the crystals of the α phase. Hence, the temperature dependence of the magnetic susceptibility of the crystals of the β phase is described by a singlet–triplet activation model

$$\chi_{singlet-triplet} = \frac{C}{T}\,\frac{4\exp(-2J/T)}{1 + 3(-2J/T)},$$

where J is the singlet–triplet splitting.

The best agreement is achieved at $2J = 140$ K.[106] Figure 24 shows the temperature dependences of the magnetic susceptibility of both phases of complex **4**. As can be seen from Fig. 24, the dependences are very similar. However, the statistical data, which would allow the authors to give preference to the spin-ladder model for the α phase and the singlet–triplet activation model for the β phase, were not given in the study.[106] Hence, the interpretation of the α phase of complex **4** as a spin ladder is not sufficiently well justified. To support the latter fact, it is necessary to study its microscopic properties of the α phase of complex **4** by neutron scattering, NMR spectroscopy, and muon spin resonance (μSR).

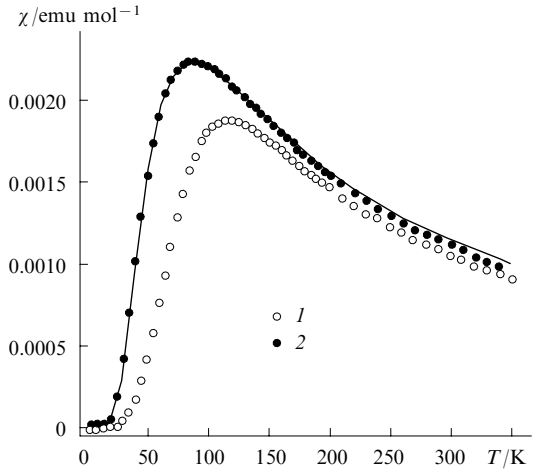


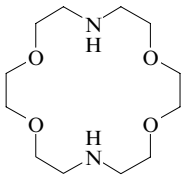
Figure 24. Temperature dependences of the magnetic susceptibility of the α (*1*) and β (*2*) phases of the $[(PhH_3N^+)\subset$(18-crown-6)$][Ni(dmit)_2]$ complex (**4**).[106]

To confirm the validity of this interpretation, the authors of the study [106] investigated crystals of the α phase of complex **4** by ^{1}H NMR spectroscopy.[108] In particular, they measured the nuclear spin–lattice relaxation time T_1^{-1}. At low temperatures, the temperature dependence of the relaxation time has two components due, apparently, to different proton states. A sharp decrease in the relaxation time at temperatures below 50 K is indicative of the formation of a spin gap. The temperature dependence of the time T_1^{-1} at low temperatures is described by the following equation

$$T_1^{-1} \sim \exp\left(-\frac{\Delta_{T_1}}{kT}\right),$$

from which the values 210 and 200 K are obtained for Δ_{T_1}. These values are in good agreement with the spin gap at 190 K determined by magnetic measurements.

1,10-Diaza-18-crown-6



was used for the synthesis of the $[K^+\subset$(1,10-diaza-18-crown-6)$][Ni(dmit)_2]$ complex (**5**) and the isostructural $[Rb^+$((1,10-diaza-18-crown-6)$][Ni(dmit)_2]$ complex (**6**).[109] In the crystals of both complexes, the $[Ni(dmit)_2]^-$ anions are extended along the a axis. Hence, π–π interactions between the anions are absent; however, there is the S(1)···S(2) interaction between the sulfur atoms of the thione and thiol groups (Fig. 25).

The temperature dependence of the magnetic susceptibility is described by the one-dimensional Heisenberg antiferromagnetic model (1D AF) with the magnetic exchange energy $J/k = -24.7$ K (potassium salt) and -22.7 K (rubidium salt).[109]

The two-rung spin-ladder model was also discussed [22] based on structural and magnetic data. The authors synthesized the (RBnpy)$[Ni(dmit)_2]$ complexes [R = NO_2 (**7**), Br (**8**); RBnpy is 1-(4′-R-benzyl)pyridinium].

In the crystals of complex **7**, the $[Ni(dmit)_2]^-$ anions form dimers due to the overlap of their π systems (plane-to-plane); the dimers are linked together through the terminal sulfur atoms to form infinite chains, resulting in the formation of a two-rung spin-ladder. A similar structure was observed in the crystals of complex **8** (Fig. 26).[22]

In spite of the structural similarity, the magnetic properties of the complexes are substantially different. Thus, the magnetic susceptibility of complex **7** slightly increases as the

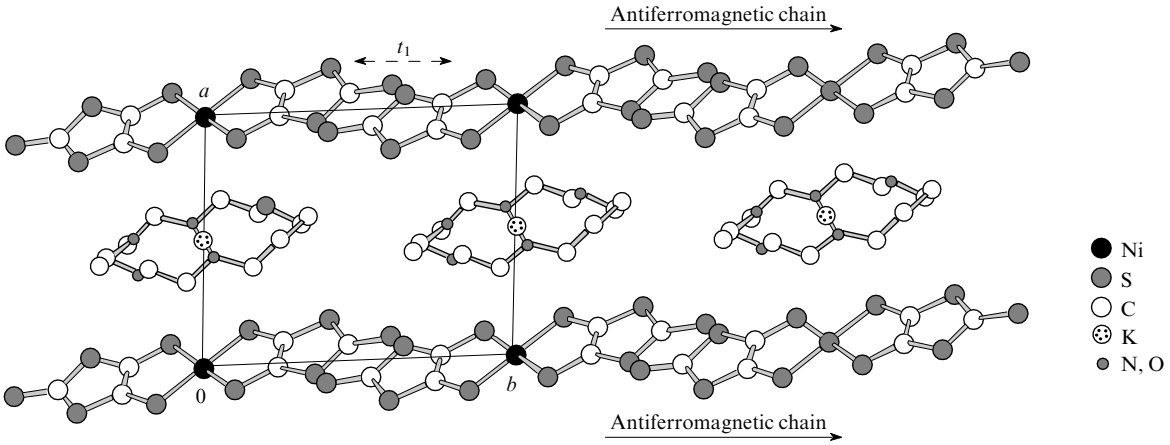


Figure 25. Projection of the crystal structure of complex **5** along the *c* axis.[109]
Antiferromagnetic chains of $[Ni(dmit)_2]^-$ anions running along the *b* axis are separated by supramolecular cations.

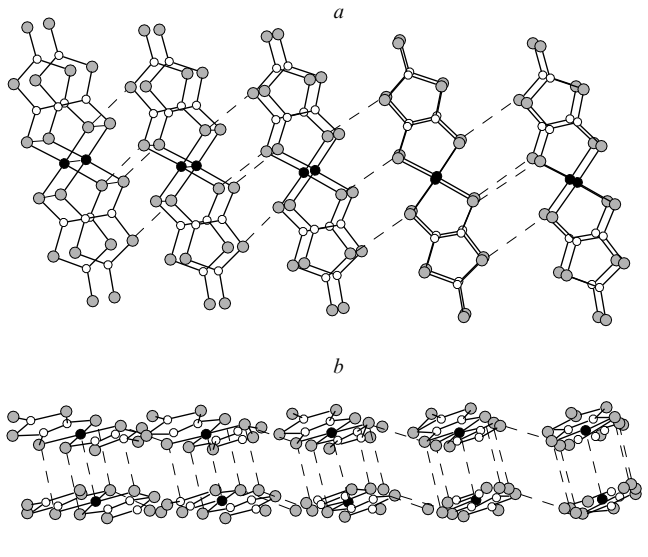


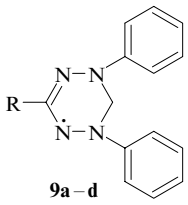
Figure 26. Spin ladder of $[Ni(dmit)_2]^-$ anions in the crystal structure of complex **8** in two projections: along the *b* axis (*a*) and along the *c* axis (*b*).[22]

temperature decreases to ~110 K. At temperatures below 110 K, the magnetic susceptibility sharply decreases. This corresponds to the phase transition with the transition temperature [determined from the dependence of $d(\chi_M T)/dT$ on T] of 100.3 K. At temperatures above 110 K, the antiferromagnetic exchange interaction between adjacent spins is dominant; at temperatures below 110 K, a spin gap is formed. It should be noted that attempts to describe the temperature dependence of the magnetic susceptibility by a model of isolated spin dimers ($s = 1/2$) or a spin-ladder model failed.[22]

The magnetic susceptibility of complex **8** increases as the temperature is lowered and reaches the maximum $\chi_M = 6.73 \times 10^{-3}$ emu mol^{-1} at $T = 16.5$ K.[22] A sharp decrease in w_M at lower temperatures is associated with antiferromagnetic ordering. It should be noted that in this case, the complexes were assigned to spin ladders based only on the crystal structure features.

Magnetically isolated π dimers were found in the crystals of the $[Ni(dmit)_2]^-$ complexes with the supramolecular 4-fluoroanilinium and 4-methylanilinium cations as complexes with 18-crown-6.[80] The $[Ni(dmit)_2]_2^{2-}$ dimers are separated by supramolecular cations. The magnetic ground state of the complexes is a spin singlet with the exchange energy in the dimer equal to −150 K.[110]

Complexes based on 1,5-diphenylverdazyl derivatives $Ct[Ni(dmit)_2]$ (Ct = **9a**–**d**) and $Ct[Ni(dmit)_2]_3$ (Ct = **9c**) were described in the study.[111]



9a–**d**

R = *N*-ethylpyridinium-4-yl (**a**),
N-ethylpyridinium-3-yl (**b**),
N-methylpyridinium-4-yl (**c**),
N-methylpyridinium-3-yl (**d**).

1,5-Diphenylverdazyl is characterized by high chemical and thermal stability. Its derivatives exhibit interesting magnetic properties, including ferromagnetism, weak ferromagnetism, antiferromagnetism, spin-Peierls transitions and spin frustration (see, for example, Ref. 112). In the crystals of the (**9a**)$[Ni(dmit)_2]$ complex, the anions form dimers, which, in turn, form a tetrameric sandwich-type structure together with the cations: $(\mathbf{9a})^+(A)-[Ni(dmit)_2]^-(A)-[Ni(dmit)_2]^-(B)-(\mathbf{9a})^+(B)$ (here, the letters A and B designate the crystallographically independent ions). According to this, the temperature dependence of the magnetic susceptibility of this complex is described by the Heisenberg Hamiltonian

$$H = -2J_1(S_1S_2 + S_3S_4) - 2J_2S_2S_3,$$

$$S_1 = S_2 = S_3 = S_4 = \frac{1}{2},$$

where J_1 is the exchange integral between the verdazyl cation and the $[Ni(dmit)_2]^-$ anion, J_2 is the exchange integral between the anions and S_i are the spins of the particles that form the tetramer. The parameters are

$2J_1/k = -780$ K and $2J_2/k = 7200$ K. The complex with cation **9c** has similar properties.

The magnetic susceptibility of the complex (**9b**)[Ni(dmit)$_2$] can be represented as the sum of two contributions:

$$\chi_M = \chi_{1D\text{-ferro}} + \chi_{S-T},$$

where the first term represents the contribution of a quasi-one-dimensional ferromagnetic linear Heisenberg spin chain and the second term corresponds to the contribution of a singlet–triplet system. For the ferromagnetic exchange, $2J/k = 2.5 \pm 1$ K; for the singlet–triplet gap, $2J/k = -320$ K.

The magnetic susceptibility of the (**9d**)[Ni(dmit)$_2$] complex can also be represented as the sum of two contributions:

$$\chi_M = C_{1D\text{-Alt}}\chi_{1D\text{-Alt}} + C_{Curie}\chi_{Curie},$$

where the first term describes the contribution of a one-dimensional antiferromagnetic alternating Heisenberg spin chain and the second term corresponds to the contribution of paramagnetic impurities. Here $2J_1/k = -165$ K and the alternating parameter $\alpha = J_2/J_1 = 0.6$.

The (**9c**)[Ni(dmit)$_2$]$_3$ complex is a narrow-band semiconductor: $\sigma_{rt} = 1.0\ \Omega^{-1}\ cm^{-1}$, and the band gap width is 0.048 eV.[112]

A series of palladate complexes $Ct_{0.5}$[Pd(dmit)$_2$] was described in the study.[113] They were characterized as Heisenberg antiferromagnets on an anisotropic triangular lattice, whose spin frustrations lead to substantial effects. The lattice anisotropy plays a decisive role at low temperatures. The temperature dependence of the magnetic susceptibility is described by the interpolation equation

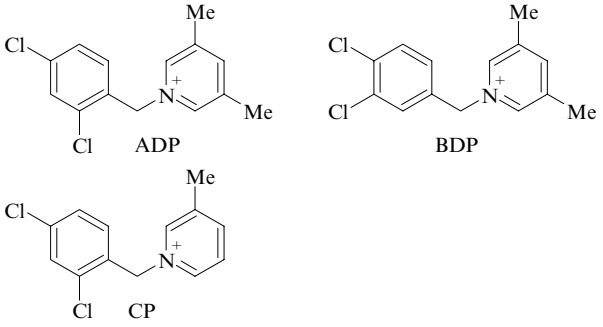
$$\chi(T) = \frac{z_{tr}J\chi_{tr}(kT/J)f(T,\Delta J) + z_{sq}\Delta J\chi_{sq}(kT/\Delta J)}{[f(T,\Delta J)+1](z_{tr}J + z_{sq}\Delta J)},$$

where χ_{tr} and χ_{sq} are the magnetic susceptibilities of the triangular (J lattice) and square (ΔJ lattice) lattices, respectively, and $f(T,\Delta J)$ is the Bose distribution function

$$f(T,\Delta J) = \frac{1}{\exp(\Delta J/kT) - 1},$$

$z_{tr} = 6$, $z_{sq} = 4$ (z is the number of nearest neighbours).

An important role of an outer-sphere cation in the formation of the magnetic structure of dmit complexes was shown.[114] The authors synthesized complexes containing the singly charged [Ni(dmit)$_2$]$^-$ anion: (ADP)$_2$[Ni(dmit)$_2$]$_2$ (**10**), BDP[Ni(dmit)$_2$]·Me$_2$CO (**11**) and (CP)$_2$[Ni(dmit)$_2$] (**12**).



In spite of insignificant structural differences of the cations, the crystal structures of the complexes are substantially different. In the crystals of complex **10**, the cations and anions together form stacks, in which the dimers of the anions are located between the dimers of the ADP cations and *vice versa*. In the crystals of complex **11**, the dimers of the [Ni(dmit)$_2$]$^-$ anions are linked together by side-by-side S···S contacts to from one-dimensional zigzag chains. In the crystals of complex **12**, there are trimers of the anions. Weak intermolecular S···Cl, C–H···Cl and C–H···S interactions stabilize the crystal structures of all three complexes and serve as magnetic coupling channels.

In accordance with this fact, the magnetic properties of these complexes also substantially depend on the nature and structure of the outer-sphere cation (Fig. 27). For complex **10**, the effective magnetic moment at 300 K (1.41 μ_B) is substantially smaller than the value expected for a single-spin system (1.73 μ_B). The magnetic moment rapidly decreases with decreasing temperature, which is typical of one-dimensional antiferromagnetic spin systems. As can be seen from Fig. 27, the magnetic susceptibility of complex **11** increases with decreasing temperature and reaches the maximum $\chi_M = 4.43 \times 10^{-3}$ emu mol^{-1} at 10.9 K. A sharp decrease in the magnetic susceptibility at lower temperatures is associated with antiferromagnetic ordering. In spite of the difference in the curves $\chi_M(T)$ (see Fig. 27 *a*,*b*), the temperature dependence $\chi_M(T)$ for both complexes can be described by the equation

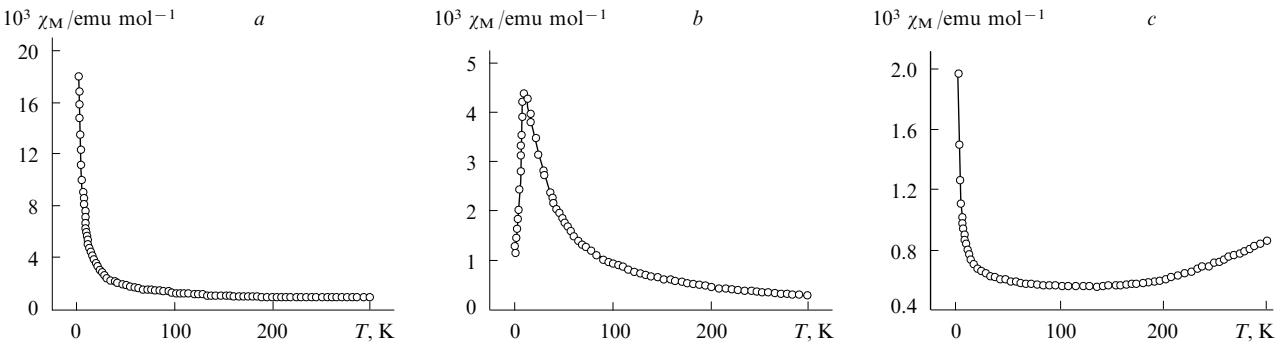


Figure 27. Temperature dependences of the molar magnetic susceptibility (χ_M) for complexes **10** (*a*), **11** (*b*) and **12** (*c*).[114]
The theoretical calculations are shown as solid lines (see the text).

$$\chi_M = \frac{\chi_{dimer}}{1 - (z_j/\beta^2 N_A g^2)\chi_{dimer}} + \frac{c}{T} + \chi_0 ,$$

where

$$\chi_{dimer} = \frac{N_A g^2 \mu_B^2}{kT}\left[3 + \exp\left(\frac{\Delta}{kT}\right)^{-1}\right],$$

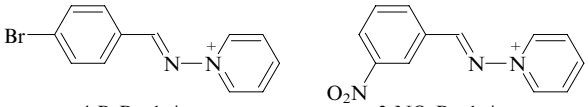
N_A is Avogadro's number and g is the g factor (Lande splitting factor).

The first, second and third terms in this equation represent the contributions of dimers, paramagnetic impurities and the possible Van Vleck paramagnetism, respectively. For complex **10**, the band gap width Δ/k = 19.8 K; for complex **11**, Δ/k = 35.2 K. The paramagnetic susceptibility of complex **12** is thermally activated and is described (minus the susceptibility of paramagnetic impurities) by the equation

$$\chi_M = \frac{\alpha \exp(-\Delta/kT)}{T}$$

with Δ/k = 1236 K.

A similar dependence of the magnetic properties of dmit complexes on the nature of outer-sphere cations was found in the study,[115] where the (4-BrBn-1-Apy)[Ni(dmit)$_2$] (**13**) and (3-NO$_2$Bn-1-Apy)[Ni(dmit)$_2$] (**14**) complexes were synthesized and characterized.



In the crystals of complex **13**, there are S···Br and S···S contacts shorter than the sum of the van der Waals radii (Fig. 28 *a*,*b*). The anions and cations form mixed stacks; however, one-dimensional wavy chains of anions are formed through S···S interactions (Fig. 28 *c*).

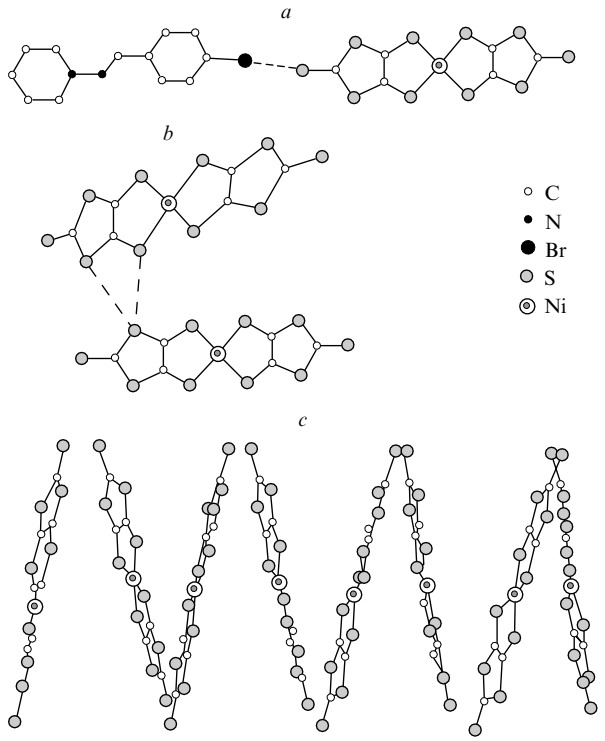


Figure 28. The S···Br (*a*) and S···S (*b*) contacts; wavy chains of the anions in the structure of complex **13** (*c*).[115]

By contrast, the anions and cations in the crystals of complex **14** form alternating two-dimensional layers parallel to the crystallographic (110) plane. Correspondingly, the magnetic properties of these complexes are different. Thus, complex **13** is a one-dimensional antiferromagnetic spin system (J/k = 66 K), whereas the magnetic susceptibility of complex **14** obeys the Curie–Weiss law (C = 0.421 emu K mol^{-1}, θ = −1.28 K, weak antiferromagnetism) throughout the temperature range under study (300–4 K).

Therefore, the magnetic properties of dmit complexes are of considerable interest. Their high variability is attributed to the effect of the nature of the central metal atom, the outer-sphere cation and the charge of the [M(dmit)$_2$]$^{n-}$ complex. However, the magnetic properties of dmit complexes are poorly known compared with their electrophysical properties. Taking into account the available data, these investigations are promising.

VI. Prospects of the practical use of isotrithionedithiolate complexes

For practical purposes, dmit complexes should be synthesized as well-faceted single crystals or films. In organic electronics, conducting Langmuir–Blodgett (L–B) films are of great interest. The advances in this field are considered in the monograph [15] referred to in the Introduction. Hence, we will mention only the most considerable results obtained mainly after the publication of this monograph.

The unusual properties of L–B films based on the *N*-(n-H$_{37}$C$_{18}$)py[Ni(dmit)$_2$] complex (**15**) with the outer-sphere *N*-octadecylpyridinium cation were described in the study.[116] Figure 29 schematically illustrates the structure of such films on the glass surface.

A bulk sample of complex **15** has low electrical conductivity, which is typical of complexes with the singly charged [M(dmit)$_2$]$^-$ anion ($\sigma_{rt} < 10^{-8}$ Ω^{-1} cm^{-1}). However, the electrical conductivity of films in the film plane is much higher [$(3.5 \pm 2.5) \times 10^{-3}$ Ω^{-1} cm^{-1}]. This fact remains unclear. The authors did not rule out the unintentional doping in the course of the preparation of L–B films, although the effect of the surface tension forces on the structure of the anionic layer is quite probable.

In 2000 the sensational study [24] on the superconductivity of L–B films based on dmit complexes was published. The authors of the study investigated the complex value of the magnetic susceptibility

$$\chi = \chi' + i\chi''$$

of L–B films based on the (n-H$_{29}$C$_{14}$)$_2$Me$_2$N[Ni(dmit)$_2$] complex (**16**). The diamagnetic transition of the real part of the magnetic susceptibility was observed, whereas the imaginary part underwent a weak jump at 3.9 K. This indicates the formation of a Meissner phase. In other words, the transition to the superconducting state occurs at T_C = 3.9 K.

More recently, the superconducting nature of the transition of complex **16** at 3.9 K was confirmed.[117] The diamagnetism was observed in a weak field (0.1 mT) at 4 K. In a magnetic field of 60 mT, the transition temper-

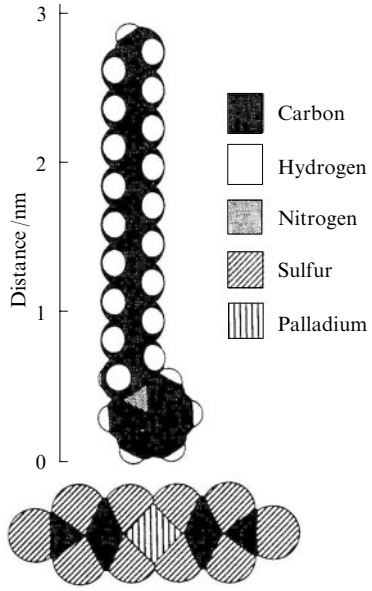
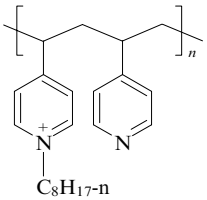


Figure 29. Structure of the Langmuir–Blodgett film based on complex **15**.[116]

ature is shifted to 3.4 K, which is typical of the transition to the superconducting state.

In the study,[118] the superconducting nature of the transition was confirmed by direct electrophysical measurements. The resistance of L–B films of complex **16** at room temperature decreases with increasing pressure; it is reduced by a factor of 6 under a pressure of 0.7 GPa. A pronounced decrease in the resistance is observed at 1.4 K under the same pressure, whereas under normal pressure, the resistance decreases at temperatures below 0.85 K followed by a weak increase at $T < 0.65$ K.

Very smooth and uniform films with a thickness of 3–5-μm were prepared by electrochemical deposition of the PVOP[M(dmit)$_2$] complexes (M = Ni, Pd).[119]

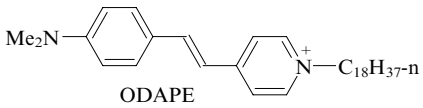


PVOP

The electrical conductivity of the starting complexes was determined on pelleted samples and is 3.2×10^{-4} and 4.0×10^{-4} Ω^{-1} cm^{-1}, respectively.[119] However, films of these complexes behave as semiconductors (the electrical conductivities at room temperature were not reported). The authors believed that this is due to the partial oxidation of the complexes in the course of electrochemical deposition.

The dmit complexes, whose structures contain cationic channels, are potentially interesting as materials for microelectronics.[120, 121] The authors of these studies synthesized a series of complexes of the composition [(Ct$^+$)$_x$-18-crown-6).[Ni(dmit)$_2$], (Ct$^+$-18-crown-6)(H$_2$O)$_x$(MeCN)$_{1.5-x}$].[Ni(dmit)$_2$], ($x = 1$ for Ct = Li, 0.5 for Ct = Na) and (Ct$^+$-18-crown-6)[Ni(dmit)$_2$] (Ct = Li, Na, K, Rb and Cs). The structures of the complexes contain ionic channels due to which alkali metal cations have particular mobility. Some of these complexes exhibit high electrical conductivity ($\sigma_{rt} \approx 10-30$ Ω^{-1} cm^{-1}). At high temperatures, the conductivity is virtually temperature-independent. The one-dimensional electronic structure is strongly influenced by the static and dynamic structure of ionic channels. Sodium salts behave as semiconductors at room temperature, and their magnetic properties are described by a one-dimensional disordered antiferromagnetic chain model. On the other hand, the caesium complex exhibits metallic properties with $2k_F$ instability at room temperature (Peierls instability). The lithium complex shows a sharp transition from the high-temperature metallic phase to the one-dimensional antiferromagnetic semiconductor phase. This transition is related to the freezing of the Li$^+$ ion motion in channels at low temperatures. Unfortunately, experiments on the determination of the possible contribution of the superionic conductivity to the electrical conductivity were not performed in the studies.[120, 121] We found for the first time a similar hybrid electronic–superionic organic conductor in the crystals of the (ET)Ag$_x$I$_8$ radical cation salt.[122]

The photoelectric properties of dmit complexes are also of interest. It was shown [123] that hemicyanine dyes belong to nonlinear optical materials because they exhibit high second-order hyperpolarizability. More recently, it was found [124] that these compounds can generate a photocurrent with quantum yields of 0.22%–0.50%. Hence, it is of interest to synthesize dmit complexes containing ODAPE ions as outer-sphere cations.



ODAPE

Complexes of the composition (ODAPE)$_2$[M(dmit)$_2$] (M = Cd, Ni) were characterized in the study.[125] It was found that these complexes also belong to nonlinear optical materials and can generate a photocurrent. In the case of the (ODAPE)$_2$[Cd(dmit)$_2$] complex, the quantum yield is 1.1%, *i.e.*, it is five times higher than that of the iodide (ODAPE)I. The second-order nonlinear optical polarizability of this complex ($\chi_{zzz} = 149.8$ pm V^{-1}) is also higher than that of (ODAPE)I. A remarkable feature of the (ODAPE)$_2$[M(dmit)$_2$] complexes is that they can form Langmuir–Blodgett films.[125]

Studies performed in the last decade showed that dmit complexes can exhibit a superfast optical response and have large third-order nonlinear optical effects.[16, 126–129] For example, the (Pr$^n_4$N)$_2$[Cu(dmit)$_2$] complex (**17**), whose crystals have a three-dimensional network of C–H···S hydrogen bonds, was described.[128] This complex is a rare example of dmit cuprates, in which the [Cu(dmit)$_2$]$^{2-}$ anion is almost planar. As mentioned in Section III, the twisted conformation of this anion is only slightly more stable than the planar conformation (by 0.08 eV) and, consequently, the Madelung energy gain in the crystal can compensate this difference. The nonlinear optical properties of complex **17** were studied [128] in an acetone solution (5×10^{-4} mol litre^{-1}) by the picosecond Z-scan technique at 1064 nm. Figure 30 shows the Z-scan curves. As can be seen from Fig. 30, complex **17** exhibits reverse saturation absorption and self-defocusing. The second-order molecular hyperpolarizability $\gamma = (1.8 \pm 0.2) \times 10^{-30}$ stat units.

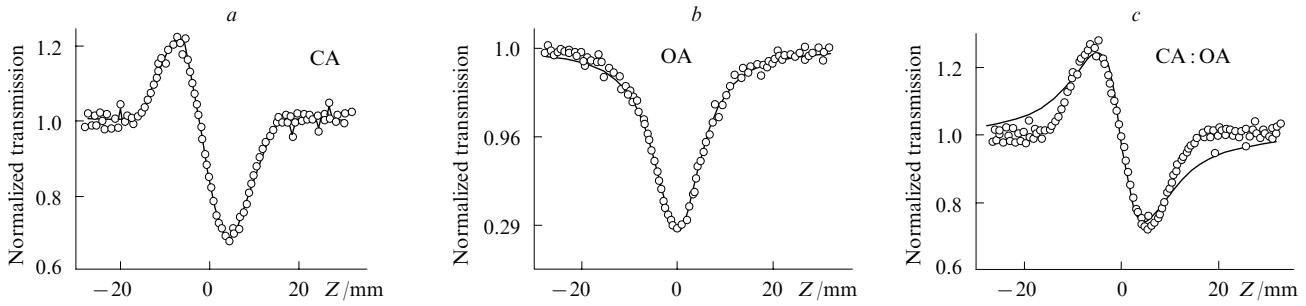


Figure 30. Closed-aperture (CA) (*a*) and open-aperture (OA) (*b*) normalized *Z*-scan curves for complex **17** in acetone (5×10^{-4} mol litre^{-1}); the result of the extraction of the curve *b* from the curve *a* (*c*).[128]
The solid line in Fig. *c* represents the theoretical fitting.

* * *

In the early 1970s, dmit complexes attracted attention as materials for the synthesis of tetrathiafulvalene derivatives, which are starting compounds for the preparation of organic metals and superconductors, *i.e.*, they played only an auxiliary role. More recently, it was found that synthetic metals and superconductors can be prepared based on mixed-valence dmit complexes. In recent years, the ability of these complexes to form magnetically ordered structures, such as quasi-one-dimensional and quasi-two-dimensional magnets and spin ladders, has been discovered and extensively investigated. It was found that these compounds have nonlinear optical and photoelectric properties. Undoubtedly, the chemistry of dmit complexes will bring many surprises because the properties of dmit complexes can be varied in a very broad range from dielectric materials with a broad band gap width to superoconductors, from diamagnets to compounds with temperature-independent paramagnetism, due to changes in the formal oxidation state of the central metal atom and variation in the nature of the outer-sphere cation.

References

1. G Steimecke, R Kirmse, E Hoyer *Z. Chem.* **15** 28 (1975)
2. S Wawzonek, S M Heilmann *J. Org. Chem.* **39** 511 (1974)
3. P Karrer *Kurs Organicheskoi Khimii* (The Course of Organic Chemistry) (Leningrad: Goskhimizdat, 1960)
4. E Fujita *Coord. Chem. Rev.* **185–186** 373 (1999)
5. T Ishiguro, K Yamaji *Organic Superconductors* (Berlin: Springer, 1990)
6. J M Williams, J R Ferraro, R J Thorn, K D Carlson, U Geiser, H H Wang, A M Kini, M-H Whangbo *Organic Superconductors (Including Fullerenes)* (Englewood Cliffs, NJ: Prentice-Hall, 1992)
7. O N Kazheva, G G Alexandrov, A V Kravchenko, V A Starodub, I A Lobanova, I B Sivaev, V I Bregadze, L V Titov, L I Buravov, O A Dyachenko *J. Organomet. Chem.* **694** 2336 (2009)
8. V Bregadze, I Sivaev, I Lobanova, O Kazheva, G Alexandrov, A Kravchenko, V Starodub, L Buravov, L Titov, O Dyachenko *J. Chem. Sci.* **122** 37 (2010)
9. L Brossard, M Ribault, M Bousseau, L Valade, P Cassoux *C. R. Acad. Sci., Ser. II* **302** 205 (1986)
10. A Kobayashi, H Kobayashi, A Miyamoto, R Kato, R A Clark, A E Underhill *Chem. Lett.* **20** 2163 (1991)
11. A Kobayashi, A Miyamoto, R Kato, A Sato, H Kobayashi *Bull. Chem. Soc. Jpn.* **71** 997 (1998)
12. P Cassoux *Coord. Chem. Rev.* **185–186** 213 (1999)
13. A E Pullen, R-M Olk *Coord. Chem. Rev.* **188** 211 (1999)
14. E Canadell *Coord. Chem. Rev.* **185–186** 629 (1999)
15. *Dithiolene Chemistry. Synthesis, Properties, and Applications* (Eds D K Karlin, E I Stiefel) (Hoboken: Wiley, 2004)
16. C-M Liu, D-Q Zhang, Y-L Song, C-L Zhan, Y-L Li, D-B Zhu *Eur. J. Inorg. Chem.* 1591 (2002)
17. Q Ren, X Zhang, X-B Sun, X-Q Wang, W-F Guo, H-L Yang, F-J Zhang, D Xu *Proc. SPIE* **6839** 68391A (2007)
18. P Romaniello, F Lelj *Chem. Phys. Lett.* **372** 51 (2003)
19. P Aloukos, S Couris, J B Koutselas, G C Anyfantis, G C Papavassiliou *Chem. Phys. Lett.* **428** 109 (2006)
20. C Zhang, Y Song, X Wang *Coord. Chem. Rev.* **251** 111 (2007)
21. C Rovira *Chem.–Eur. J.* **6** 1723 (2000)
22. Y Chen, G Liu, Y Song, H Xu, X Ren, Q Meng *Polyhedron* **24** 2269 (2005)
23. M C Aragoni, M Arca, F A Devillanova, F Isaia, V Lippolis, A Mancini, L Pala, G Verani, T Agostinelli, M Caironi, D Natali, M Sampietro *Inorg. Chem. Commun.* **10** 191 (2007)
24. Y F Miura, M Horikiri, S-H Saito, M Sugi *Solid State Commun.* **113** 603 (2000)
25. O Ya Neiland, Ya Ya Katsens, Ya N Kreitsberga *Zh. Org. Khim.* **25** 658 (1989) [a]
26. V A Starodub, V P Batulin, M A Obolenskii *Koord. Khim.* **20** 677 (1994) [b]
27. V A Starodub, T N Zinenko, A R Kazachkov *Synth. Met.* **131** 49 (2002)
28. T N Zinenko, V A Starodub, A R Kazachkov *Koord. Khim.* **29** 428 (2003) [b]
29. C P Galloway, D D Doxsee, D Fenske, T B Rauchfuss, S R Wilson, X Yang *Inorg. Chem.* **33** 4537 (1994)
30. H Li, D Zhang, B Zhang, Y Yao, W Xu, D Zhu, Z Wang *J. Mater. Chem.* **10** 2063 (2000)
31. N Svenstrup, J Becher *Synthesis* 215 (1995)
32. A M Kini, J P Parakka, U Geiser, H-H Wang, F Rivas, E DiNino, S Thomas, J D Dudek, J M Williams *J. Mater. Chem.* **9** 883 (1999)
33. P Cassoux, L Valade, H Kobayashi, A Kobayashi, R A Clark, A E Underhill *Coord. Chem. Rev.* **110** 115 (1991)
34. L Valade, J-P Legros, M Bousseau, P Cassoux, M Garbauskas, L V Inerrante *J. Chem. Soc., Dalton Trans.* 783 (1985)
35. L Valade, M Bousseau, A Gleizes, P Cassoux *J. Chem. Soc., Chem. Commun.* 110 (1983)
36. D Mentzafos, A Hountas, A Terzis *Acta Crystallogr., Sect. C* **44** 1550 (1988)
37. V A Starodub, Doctoral Thesis in Chemical Sciences, Khar'kov National University, Khar'kov 1994
38. R Kirmse, J Stach, W Dietzsch, G Steimecke, E Hoyer *Inorg. Chem.* **19** 2679 (1980)
39. V A Starodub, V N Baumer, M A Obolenskii *Koord. Khim.* **13** 1403 (1987) [b]

40. V N Baumer, V A Starodub, G E Tarasova *Kristallografiya* **34** 102 (1989) [c]
41. F Cotton, G Wilkinson *Advanced Inorganic Chemistry. A Comprehensive Text* (New York: Interscience, Wiley, 1972)
42. H B Gray, E Billig *J. Am. Chem. Soc.* **85** 2019 (1963)
43. G N Schrauzer, V P Mayweg *J. Am. Chem. Soc.* **87** 1483 (1965)
44. E I Stiefel, J H Waters, E Billig, H B Gray *J. Am. Chem. Soc.* **87** 3016 (1965)
45. G N Schrauzer, V P Mayweg *J. Am. Chem. Soc.* **87** 3585 (1965)
46. R Williams, E Billig, J H Waters, H B Gray *J. Am. Chem. Soc.* **88** 43 (1966)
47. A Davison, N Edelstein, R H Holm, A H Maki *J. Am. Chem. Soc.* **86** 2799 (1964)
48. K P Butin, E K Beloglazkina, N V Zyk *Russ. Chem. Rev.* **74** 531 (2005); *Usp. Khim.* **74** 585 (2005)
49. V A Starodub, V N Uvarov *Koord. Khim.* **23** 117 (1997) [b]
50. J P Cornelissen, R Le Loux, J Jansen, J G Haasnoot, J Reedijk, E Horn, A L Spek, B Pomaredzh, J-P Legros, D Reefman *J. Chem. Soc., Dalton Trans.* 2911 (1992)
51. V E Shklover, S S Nagapetyan, Yu T Struchkov *Russ. Chem. Rev.* **59** 686 (1990); *Usp. Khim.* **59** 1179 (1990)
52. K I Pokhodnya, C Faulmann, I Malfant, R Andreu-Solano, P Cassoux, A Mlayah, D Smirnov, J Leotin *Synth. Met.* **103** 2016 (1999)
53. U Fano *Phys. Rev.* **124** 1866 (1961)
54. V A Starodub, A V Kravchenko, A R Kazachkov, V V Khotkevich, A V Khotkevich, O S Pyshkin, G V Kamarchuk *Funct. Mater.* **10** 739 (2003)
55. M V Belousov, A M Vainrub, R M Vlasova, V N Semkin *Fiz. Tv. Tela* **20** 107 (1978) [d]
56. L P Gor'kov, E I Rashba *Solid State Commun.* **27** 1211 (1978)
57. T Kondow, T Sakata *Phys. Status Solidi, A* **6** 551 (1971)
58. V M Yartsev *Zh. Prikl. Spektrosk.* **34** 513 (1981) [e]
59. V A Starodub, T B Drushlyak, L A Sleta *Int. J. Quantum Chem.* **24** 149 (1983)
60. R Ramakumar, Y Tanaka, K Yamaji *Phys. Rev. B* **56** 795 (1997)
61. H L Liu *Phys. Rev. B* **53** 10557 (1996)
62. H Tamura, S Tanaka, G-e Matsubayashi, W Mori *Inorg. Chim. Acta* **232** 51 (1995)
63. T Miyazaki, T Ohno *Phys. Rev. B* **59** R5269 (1999)
64. M Tamura, K Takenaka, H Takagi, S Sugai, A Tajima, R Kato *Chem. Phys. Lett.* **411** 133 (2005)
65. G B Carpenter, G S Clark, A L Rieger, P H Rieger, D A Sweigart *J. Chem. Soc., Dalton Trans.* 2903 (1994)
66. F Matsuda, H Tamura, G-e Matsubayashi *Inorg. Chim. Acta* **295** 239 (1999)
67. G-e Matsubayashi, K Takagashi, T Tanaka *J. Chem. Soc., Dalton Trans.* 967 (1988)
68. D-Y Noh, A E Underhill, M B Hursthouse *Chem. Commun.* 2211 (1997)
69. S Sun, P Wu, D Zhu *Synth. Met.* **88** 243 (1997)
70. M Dressel *Naturwissenschaften* **90** 337 (2003)
71. M L Mercuri, P Deplano, L Pilia, A Serpe, F Artizzu *Coord. Chem. Rev.* **254** 1419 (2010)
72. O Lindqvist, L Sjllin, J Sieler, G Steimecke, E Hoyer *Acta Chem. Scand. Ser. A* **33** 445 (1979)
73. O Lindqvist, L Andersen, J Sieler, G Steimecke, E Hoyer *Acta Chem. Scand., Ser. A* **36** 855 (1982)
74. N Bartlett, E M McCarron, B W McQuillan, T E Thompson *Synth. Met.* **1** 221 (1980)
75. R E Peierls *Quantum Theory of Solids* (London: Oxford University Press, 1955)
76. V A Starodub, I V Krivoshei *Russ. Chem. Rev.* **51** 439 (1982); *Usp. Khim.* **51** 764 (1982)
77. H Tajima, T Naito, M Tamura, A Takahashi, S Toyoda, A Kobayashi, H Kuroda, R Kato, H Kobayashi, R A Clark, A E Underhill *Synth. Met.* **42** 2417 (1991)
78. R Kato, Y-L Liu, S Aonuma, H Sawa *Solid State Commun.* **98** 1021 (1996)
79. A Kobayashi, H Kini, Y Sasaki, K Murata, R Kato, H Kobayashi *J. Chem. Soc., Faraday Trans.* **86** 361 (1990)
80. R Kato, N Tajima, A Tajima, M Tamura, J Yamaura *Synth. Met.* **137** 1233 (2003)
81. H Kino, H Fukuyama *J. Phys. Soc. Jpn.* **64** 2726 (1995)
82. H Tajima, T Naito, M Tamura, A Kobayashi, H Kuroda, R Kato, H Kobayashi, R A Clark, A E Underhill *Solid State Commun.* **79** 337 (1991)
83. Q Fang, H Lei, Z Liu, B Zhang, Y Sun, T C W Mak *Sci. China, Ser. B* **45** 97 (2002)
84. T Nakamura, A E Underhill, A T Coomber, R H Friend, H Tajima, A Kobayashi, H Kobayashi *Synth. Met.* **70** 1061 (1995)
85. Z S Li, S Matsuzaki, R Kato, H Kobayashi, A Kobayashi, M Sano *Chem. Lett.* 1105 (1986)
86. D V Ziolkovskiy, A V Kravchenko, V A Starodub, O N Kazheva, A V Khotkevich *Funct. Mater.* **12** 577 (2005)
87. L Valade, J-P Legros, P Cassoux, F Kubel *Mol. Cryst. Liq. Cryst.* **140** 335 (1986)
88. A E Pullen, C Faulmann, H-L Liu, D B Tanner, K A Abboud, J R Reynolds *Inorg. Chim. Acta* **282** 90 (1998)
89. E M Sokolovskaya, L S Guzei *Metallokhimiya* (Metallochemistry) (Moscow: Moscow State University, 1986)
90. M Trömel, S Hübner *Z. Kristallogr.* **215** 429 (2000)
91. S S Batsanov *Neorg. Mater.* **37** (1) 30 (2001) [f]
92. Q Fang, W Xu, H Lei, G Xue, H Chen, C Xu, C Jia, D Zhang *Sci. China, Ser. B* **46** 595 (2003)
93. R Drago *Physical Methods in Chemistry* (Philadelphia: Saunders, 1977)
94. T Hirose, H Imai, T Naito, T Inabe *J. Solid State Chem.* **168** 535 (2002)
95. A J Epstein, E M Conwell, J S Miller, in *Synthesis and Properties of Low-Dimensional Materials* (Eds J S Miller, A J Epstein) (New York: New York Academy Sciences, 1978) p. 183
96. K Tomono, K Ogawa, Y Sasaki, K Miyamura *Inorg. Chim. Acta* **361** 269 (2008)
97. M Uruichi, K Yakushi, Y Yamashita *J. Mater. Chem.* **10** 2716 (2000)
98. Y Misaki, T Kaibuki, M Taniguchi, K Tanaka, T Kawamoto, T Mori, T Nakamura *Chem. Lett.* **29** 1274 (2000)
99. K Takimiya, Y Kataoka, Y Aso, T Otsubo, H Fukuoka, S Yamanaka *Angew. Chem., Int. Ed.* **40** 1122 (2001)
100. H Nishikawa, T Morimoto, T Kodama, I Ikemoto, K Kikuchi, J Yamada, H Yoshino, K Murata *Synth. Met.* **133**–**134** 193 (2003)
101. E I Zhilyaeva, S A Torunova, R N Lyubovskaya, G A Mousdis, G C Papavassiliou, J A A J Perenboom, S I Pesotskii, R B Lyubovskii *Synth. Met.* **140** 151 (2004)
102. Y Kashimura, Y Okano, J-I Yamaura, R Kato *Synth. Met.* **103** 2123 (1999)
103. S V Vitushkina, D V Ziolkovskiy, V A Starodub, I A Presniakov, A V Sobolev, M Kajňaková, A Radvákova, A Feher *Res. Lett. Inorg. Chem.* ID 243296 (2009)
104. A S Davydov *Teoriya Tverdogo Tela* (The Theory of Solid) (Moscow: Nauka, 1976)
105. N Robertson, L Cronin *Coord. Chem. Rev.* **227** 93 (2002)
106. S Nishihara, T Akutagawa, T Hasegawa, S Fujiyama, Tosh Nakamura, Tak Nakamura *J. Solid State Chem.* **168** 661 (2002)
107. M Troyer, H Tsunetsugu, D Würtz *Phys. Rev. B* **50** 13515 (1994)
108. S Nishihara, T Akutagawa, T Hasegawa, Tak Nakamura, S Fujiyama, Tosh Nakamura *Synth. Met.* **137** 1279 (2003)
109. T Akutagawa, T Nakamura *Coord. Chem. Rev.* **226** 3 (2002)
110. S Nishihara, X M Ren, T Akutagawa, T Nakamura *Polyhedron* **24** 2844 (2005)
111. Kaz Mukai, D Shiba, Kyo Mukai, K Yoshida, H Hisatou, K Ohara, Y Hosokoshi, N Azuma *Polyhedron* **24** 2513 (2005)

112. K Mukai, M Matsubara, H Hisatou, Y Hosokoshi, K Inoue, N Azuma *J. Phys. Chem. B* **106** 8632 (2002)
113. M Tamura, R Kato *Polyhedron* **24** 2817 (2005)
114. G-X Liu, H Yang, W Guo, Y Liu, R-Y Huang, S Nishihara, X-M Ren *Polyhedron* **29** 2916 (2010)
115. H Zhang, H-R Zhao, X-M Ren, H-B Duan, Z-F Tian, Q-J Meng *Inorg. Chim. Acta* **363** 3530 (2010)
116. C Pearson, Z A Ibrahim, A S Dhindsa, A S Batsanov, M R Bryce, J A K Howard, M C Petty, A E Underhill *J. Mater. Chem.* **8** 387 (1998)
117. Y F Miura, M Horikiri, S Tajima, T Wakaita, S-H Saito, M Sugi *Synth. Met.* **133**–**134** 663 (2003)
118. Y F Miura, M Hedo, Y Uwatoko, S-H Saito, M Sugi *Synth. Met.* **137** 1311 (2003)
119. R Shen, W Xu, D Zhang, D Zhu *Solid State Commun.* **130** 401 (2004)
120. K Shitagami, T Akutagawa, T Hasegawa, T Nakamura, N Robertson *Acta Crystallogr., Sect. C* **57** 1271 (2001)
121. T Akutagawa, T Hasegawa, T Nakamura, S Takeda, T Inabe, K Sugiura, Y Sakata, A E Underhill *Chem.–Eur. J.* **7** 4902 (2001)
122. M A Tanatar, G O Baram, V A Bondarenko, K I Pokhodnya, V A Starodub *Teor. Eksp. Khim.* **25** 247 (1989) [g]
123. G J Ashwell, R C Hargreaves, C E Baldwin, G S Bahra, C R Brown *Nature (London)* **357** 393 (1992)
124. A D Lang, J Zhai, C H Huang, L-B Gan, Y-L Zhao, D-J Zhou, Z-D Chen *J. Phys. Chem. B* **102** 1424 (1998)
125. J Zhai, C Huang, T-X Wei, L Gan, H Cao *Polyhedron* **18** 1513 (1999)
126. S Wang, W Huang, T Zhang, H Yang, Q Gong, Y Okuma, M Horikiri, Y F Miura *Appl. Phys. Lett.* **75** 1845 (1999)
127. J Day, G-Q Bian, X Wang, Q-F Xu, M-Y Zhou, M Munakata, M Maekawa, M-H Tong, Z-R Sun, H-P Zeng *J. Am. Chem. Soc.* **122** 11007 (2000)
128. W F Guo, X B Sun, J Sun, W T Yu, X Q Wang, G H Zhang, D Xu *Cryst. Res. Technol.* **42** 522 (2007)
129. H Yang, X Wang, Q Ren, G Zhang, X Sun, L Feng, S Wang, Z Wang *J. Opt. A: Pure Appl. Opt.* **7** 510 (2005)

[a] — *Russ. J. Org. Chem. (Engl. Transl.)*
[b] — *Russ. J. Coord. Chem. (Engl. Transl.)*
[c] — *Crystallogr. Rep. (Engl. Transl.)*
[d] — *Phys. Solid State (Engl. Transl.)*
[e] — *J. Appl. Spectrosc. (Engl. Transl.)*
[f] — *Inorg. Mater. (Engl. Transl.)*
[g] — *Theor. Exp. Chem. (Engl. Transl.)*